https://doi.org/10.5194/bg-2021-19
Preprint. Discussion started: 1 February 2021
© Author(s) 2021. CC BY 4.0 License.

Biogeosciences Discussions Open Access EGU

Temporal variability and driving factors of the carbonate system in the Aransas Ship Channel, TX: A time-series study

Melissa R. McCutcheon[1], Hongming Yao[1,#], Cory J. Staryk[1], Xinping Hu[1]

[1] Harte Research Institute for Gulf of Mexico Studies, Texas A&M University – Corpus Christi, TX 78412, USA
[#] current address: Shenzhen Engineering Laboratory of Ocean Environmental Big Data Analysis and Application, Shenzhen Institute of Advanced Technology, Chinese Academy of Sciences, Shenzhen 518055, China

_____

Correspondence to: Melissa R. McCutcheon (melissa.mccutcheon@tamucc.edu)

Keywords: pCO_2, acidification, diel variability, seasonal variability, autonomous sensors

https://doi.org/10.5194/bg-2021-19
Preprint. Discussion started: 1 February 2021
© Author(s) 2021. CC BY 4.0 License.

Biogeosciences Discussions

Abstract

Estuaries are complex systems with substantial heterogeneity in water chemistry, including carbonate chemistry parameters such as pH and partial pressure of CO_2 (pCO_2), because of the diversity of co-occurring biogeochemical processes. To better understand estuarine acidification and air-sea CO_2 fluxes from estuaries, it is important to study baseline variability and driving factors of carbonate chemistry. Using both discrete bottle sample collection (2014-2020) and hourly sensor measurements (2016-2017), we explored temporal variability, from diel to interannual scales, in the carbonate system (specifically pH and pCO_2) at the Aransas Ship Channel located in northwestern Gulf of Mexico. Using other co-located environmental sensors, we also explored the driving factors of that variability. Both sampling methods demonstrated significant seasonal variability at the location, with highest pH (lowest pCO_2) in the winter and lowest pH (highest pCO_2) in the summer. Significant diel variability was also evident from sensor data, but the time of day with elevated pCO_2/depressed pH was not consistent across the entire monitoring period, sometimes reversing from what would be expected from a biological signal. Though seasonal and diel fluctuations were smaller than many other areas previously studied, carbonate chemistry parameters were among the most important environmental parameters to distinguish between time of day and between seasons. It is evident that temperature, biological activity, and tide level (despite the small tidal range) are all important controls on the system, with different controls dominating at different time scales. The results suggest that the controlling factors of the carbonate system may not be exerted equally on both pH and pCO_2 on diel timescales, causing separation of their diel or tidal relationships during certain seasons. Despite known temporal variability

https://doi.org/10.5194/bg-2021-19
Preprint. Discussion started: 1 February 2021
© Author(s) 2021. CC BY 4.0 License.


on shorter timescales, discrete sampling was generally representative of the average carbonate system and average air-sea CO_2 flux on a seasonal and annual basis based on comparison with sensor data.

1. Introduction

Estuaries, the dynamic environments where the coast and freshwater inflows meet the ocean, are economically and ecologically important because they are biological hotspots, but they are also heavily influenced by anthropogenic activity. Because of the diversity of co-occurring biogeochemical processes, estuaries experience substantial spatial and temporal heterogeneity in water quality and chemistry, including carbonate chemistry parameters such as pH and partial pressure of CO_2 (pCO_2) (Hofmann et al., 2011; Waldbusser and Salisbury, 2014). Carbonate chemistry, or the speciation of inorganic carbon in seawater, is important for two main reasons. First, CO_2 acidifies seawater, whether it is a result of uptake from the atmosphere (generally acknowledged as ocean acidification, or OA) or it is produced by biogeochemical processes in the water (that may intensify or alleviate the effects of OA). This is problematic because acidification can negatively affect marine organisms, especially those that construct calcium carbonate shells and skeletons (Barton et al., 2015; Bednaršek et al., 2012; Ekstrom et al., 2015; Gazeau et al., 2007; Gobler and Talmage, 2014). Second, the ocean contributes substantially to the global carbon budget, which is important to understand because of climate change implications. Despite the small surface area of coastal waters relative to the global ocean, coastal waters are recognized as important contributors in global carbon cycling (Borges, 2005; Cai, 2011; Laruelle et al., 2018).

https://doi.org/10.5194/bg-2021-19
Preprint. Discussion started: 1 February 2021
© Author(s) 2021. CC BY 4.0 License.


While open ocean environments are relatively well studied and understood regarding carbonate chemistry, acidification, and air-sea CO_2 fluxes, large uncertainties remain in estuarine environments. Estuaries are challenging to fully understand because of the heterogeneity between and within estuaries that is driven by diverse processes operating on different time scales such as river discharge, nutrient and organic matter loading, stratification, and coastal upwelling (Jiang et al., 2013; Mathis et al., 2012). The traditional sampling method for carbonate system characterization involving discrete water sample collection and laboratory analysis is known to lead to biases in average pCO_2 and CO_2 flux calculations due to daytime sampling that neglects to capture diel variability (Li et al., 2018). Mean diel ranges in pH can exceed 0.1 unit and single day ranges can exceed 1 pH unit, with especially high diel variability in biologically productive areas or areas with higher mean pCO_2 (Challener et al., 2015; Cyronak et al., 2018; Schulz and Riebesell, 2013; Semesi et al., 2009; Yates et al., 2007). These diel ranges can far surpass the magnitude of the changes in open ocean surface waters that have occurred since the start of the industrial revolution and rival spatial variability in productive systems, indicating their importance for a full understanding of the carbonate system.

Despite the need for high-frequency measurements, sensor deployments have been limited in estuarine environments (especially compared to their extensive use in the open ocean) because of the challenges associated with varying conditions, biofouling, and sensor drift (Sastri et al., 2019). Carbonate chemistry monitoring in the Gulf of Mexico (GOM), and especially its estuaries, has been relatively minimal compared to the United States east and west coasts. The GOM estuaries, where this study takes place,

https://doi.org/10.5194/bg-2021-19
Preprint. Discussion started: 1 February 2021
© Author(s) 2021. CC BY 4.0 License.


currently have less exposure to concerning levels of acidification than other estuaries because of their high temperatures (causing water to hold less CO_2 and support high productivity year-round) and often suitable river chemistries (i.e. relatively high buffer capacity) (McCutcheon et al., 2019; Yao et al., 2020). However, respiration-induced acidification is present in both the open GOM (e. g., subsurface water influenced by the Mississippi River Plume and outer shelf region near the Flower Garden Banks National Marine Sanctuary) and GOM estuaries, and most estuaries in the northwestern GOM have also experienced long-term acidification (Cai et al., 2011; Hu et al., 2018, 2015; Kealoha et al., 2020; McCutcheon et al., 2019; Robbins and Lisle, 2018). This known acidification as well as the relatively high CO_2 fluxes from the estuaries of the northwest GOM (which may change our understanding of global estuarine contribution to the carbon budget) illustrates the necessity to study the baseline variability and driving factors of carbonate chemistry in the region. In this study, we explored temporal variability in the carbonate system in Aransas Ship Channel—a tidal inlet in a semi-arid region of the northwestern GOM—using both discrete bottle sample collection and hourly sensor measurements, and we explored the driving factors of that variability using data from other co-located environmental sensors.

2. Materials and Methods

2.1 Location

Autonomous sensor monitoring and discrete water sample collections for laboratory analysis of carbonate system parameters were performed in the Aransas Ship Channel (27˚50'17"N, 97˚3'1"W). The Aransas Ship Channel is one of the few permanent tidal inlets that intersect a string of barrier islands and connect the GOM coastal waters

https://doi.org/10.5194/bg-2021-19
Preprint. Discussion started: 1 February 2021
© Author(s) 2021. CC BY 4.0 License.

with the lagoonal estuaries in the northwest GOM (Fig. 1). The Aransas Ship Channel provides the direct connection between the nwGOM and the Mission-Aransas Estuary (Copano and Aransas Bays) to the north and Nueces Estuary (Nueces and Corpus Christi Bays) to the south (Fig. 1). The tidal range in the region is small, with around 0.6 m tides on the open coast and less than 0.3 m in the estuaries (Montagna et al., 2011). Mission-Aransas Estuary (MAE) is fed by two small rivers, the Mission (1787 km^2 drainage basin) and Aransas (640 km^2 drainage basin) Rivers (http://waterdata.usgs.gov/), which both experience low base flows punctuated by periodic high flows during storm events. MAE has an average residence time of one year (Solis and Powell, 1999), so there is a substantial lag between time of rainfall and riverine delivery to the Aransas Ship Channel in the lower estuary. A significant portion of riverine water flowing into Aransas Bay originates from the larger rivers further northeast on the Texas coast via the Intracoastal Waterway (i.e. Guadalupe River (26,625 km^2 drainage basin) feeds San Antonio Bay and has a much shorter residence time of nearly 50 days) (Solis and Powell, 1999; USGS, 2001).

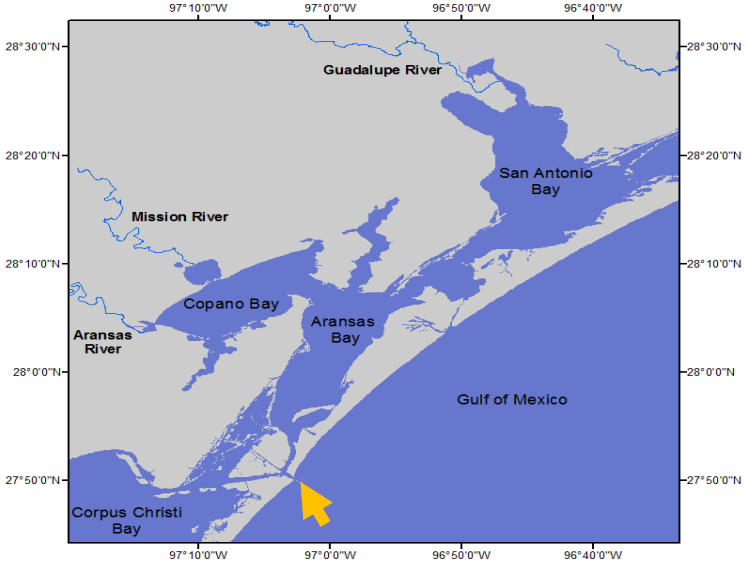

Fig 1. Location of Aransas Ship Channel where this study took place (arrow) and surrounding bay systems.

https://doi.org/10.5194/bg-2021-19
Preprint. Discussion started: 1 February 2021
© Author(s) 2021. CC BY 4.0 License.


133 *2.2 Continuous Monitoring*

134 Autonomous sensor monitoring (referred to throughout as continuous monitoring)
135 of pH and pCO_2 was conducted from Nov. 8, 2016 to Aug. 23, 2017 at the University of
136 Texas Marine Science Institute's research pier in the Aransas Ship Channel. The sensor
137 deployment was shorter than intended because the pier where the sensors were deployed
138 was destroyed in the aftermath of Hurricane Harvey in 2017. The pH data were collected
139 using an SAtlantic® SeaFET pH sensor (on total pH scale) and pCO_2 data were collected
140 using a Sunburst® SAMI-CO_2. Temperature and salinity data were measured by a YSI®
141 600OMS V2 sonde. Hourly data collected by all sensors (pH, pCO_2, salinity, and
142 temperature) were saved in the onboard data loggers and downloaded during service trips
143 to the field site. Sensor failures or pump failures occurred for short periods of time
144 throughout the deployment. Measurements were recorded on 262 individual days, with
145 176 of those days having the full set of 24 (hourly) measurements.

146 Ideally, *in-situ* sensors should be deployed under the sea surface. However, to
147 reduce the maintenance cost and effort for sensors deployed in warm water that
148 experiences intense biofouling, the sensors were set up to measure pH and pCO_2 from an
149 *ex situ* position using *in situ* seawater. Water was pumped from ~1 m below the sea
150 surface into the bottom spigot of a 100-Qt cooler that housed the SAMI-CO2 and SeaFET
151 sensors. To allow water outflow, a 1" hole was drilled at the opposite side of the spigot
152 near the top of the cooler rim, allowing water to flow back to the sea surface. The pump
153 was programmed to turn on 20 minutes before each hour, pumping more than enough
154 water to fully flush the cooler, and sensors recorded measurements on the hour. The YSI

https://doi.org/10.5194/bg-2021-19
Preprint. Discussion started: 1 February 2021
© Author(s) 2021. CC BY 4.0 License.


sonde was deployed directly into the Aransas Ship Channel inside a 2" PVC pipe at ~1 m below the sea surface.

Visits to the field site were conducted every two weeks to service all sensors and clean the cooler. Additionally, duplicate water samples were collected on the hour during service trips for quality assurance of sensor data and to check that surface water and cooler chemistries aligned. Samples were collected from the channel near the pump inlet and from the cooler that housed the sensors, and water temperature and salinity were measured using a handheld YSI data sonde. The average difference between sensor pH and laboratory pH (from the cooler) was used to establish a correction of -0.05 to the final *in-situ* pH data since the SeaFET may experience drift. The difference between the sensor pCO_2 and calculated pCO_2 is reported, but it is not used for a correction since the spectrophotometric measurements of the SAMI-CO2 should not experience drift. Sensor data were discarded from analysis during known periods of pump failure when cooler chemistry separated from that of the Aransas Ship Channel.

2.3 Discrete Sample Collection and Analysis

In addition to the discrete sample collections that occurred for quality assurance during sensor servicing visits, long-term monitoring via discrete water sample collection was conducted at the Aransas Ship Channel from May 2, 2014 to February 25, 2020. Sampling was conducted from a small vessel at a station very near to the sensor deployment every two weeks during the summer months and monthly during the winter months. Water sample collection followed standard protocol for ocean carbonate chemistry studies (Dickson et al., 2007). Ground glass borosilicate bottles (250 mL) were filled with surface water and preserved with 100 µL saturated mercury chloride ($HgCl_2$).

https://doi.org/10.5194/bg-2021-19
Preprint. Discussion started: 1 February 2021
© Author(s) 2021. CC BY 4.0 License.


Apiezon ® grease was applied to the bottle stopper, which was then secured to the bottle using a rubber band and a nylon hose clamp.

These samples were used for laboratory dissolved inorganic carbon (DIC) and pH measurements. DIC was measured by injecting 0.5 mL of sample into 1 ml 10% H_3PO_4 (balanced by 0.5 M NaCl) with a high-precision Kloehn syringe pump. The CO_2 gas produced through sample acidification was then stripped using high-purity nitrogen gas and carried into a Li-Cor infrared gas detector. DIC analyses had a precision of 0.1%. Certified Reference Material (CRM) was used to ensure the accuracy of the analysis (Dickson et al. 2003). For samples with salinity>20, pH was measured using a spectrophotometric method at 25 ± 0.1°C (Carter et al. 2003) and the Douglas and Byrne (2017) equation. Analytical precision of the spectrophotometric method for pH measurement was ±0.0004 pH units. A calibrated Orion Ross glass pH electrode was used to measure pH at 25 ± 0.1°C for samples with salinity<20, and analytical precision was ±0.01 pH units. All pH values obtained using the potentiometric method were converted to total scale at *in situ* temperature (Millero 2001). Salinity of the discrete samples was measured using a benchtop salinometer calibrated by MilliQ water and a known salinity CRM.

2.4 Data Processing and Statistical Analyses

For the discrete samples, pCO_2 was calculated using CO2Sys for Excel. Carbonate speciation calculations were done using Millero (2010) carbonic acid dissociation constants (K_1 and K_2), Dickson (1990) bisulfate dissociation constant, and Uppström (1974) borate concentration. Temporal variability was investigated in the form of seasonal and diel variability (Tables 1-2). For seasonal analysis, December to February

https://doi.org/10.5194/bg-2021-19
Preprint. Discussion started: 1 February 2021
© Author(s) 2021. CC BY 4.0 License.


was considered winter, March to May was considered spring, June to August was considered summer, and September to November was considered fall. Two-way ANOVAs were used to examine differences in parameter means between seasons, using differences between monitoring methods as the second factor (as differences between seasons may not be the same between monitoring methods, Table 3). Since there was a significant interaction in the two-way ANOVA, the differences between seasons were investigated within each monitoring method. Post-hoc multiple comparisons (between seasons within sampling types) were conducted using the Westfall adjustment (Westfall, 1997). For diel comparisons, daytime and nighttime variables were defined as 09:00-15:00 local standard time and 21:00-03:00 local standard time, respectively, based on the 6-hour periods with highest and lowest photosynthetically active radiation (PAR; data obtained from the Mission-Aransas National Estuarine Research Reserve (MANERR) at https://missionaransas.org/science/download-data. Paired *t*-tests, comparing the daytime mean with the nighttime mean on respective days, were used to look for significant differences between daytime and nighttime parameter values across the full sampling period and within each season (Table 2).

Equation 1 was used for air-water CO_2 flux calculations (Wanninkhof, 1992; Wanninkhof et al., 2009). Positive flux values indicate CO_2 emission from the water into the atmosphere (the estuary acting as a source of CO_2), and negative flux values indicate CO_2 uptake by the water (the estuary acting as a sink for CO_2).

$$F = k\, K_0\, (pCO_{2,w} - pCO_{2,a}) \quad (1)$$

https://doi.org/10.5194/bg-2021-19
Preprint. Discussion started: 1 February 2021
© Author(s) 2021. CC BY 4.0 License.


where k is the gas transfer velocity (in m d^{-1}), K_0 (in mol l^{-1} atm^{-1}) is the solubility constant of CO_2 (Weiss, 1974), and $pCO_{2,w}$ and $pCO_{2,a}$ are the partial pressure of CO_2 (in µatm) in the water and air, respectively.

We used the wind speed parameterization for gas transfer velocity (*k*) from Jiang et al. (2008) converted from cm h^{-1} to m d^{-1}, which is thought to be the best estuarine parameterization at this time (Crosswell et al., 2017) as it is a composite of *k* over several estuaries. The calculation of *k* requires a windspeed at 10 m above the surface, so windspeeds measured at 3 m above the surface were converted using the power law wind profile (Hsu, 1994; Yao and Hu, 2017). To assess uncertainty, other parameterizations with direct applications to estuaries in the literature were also used to calculate CO_2 flux (Raymond and Cole 2001; Ho et al. 2006). We note that parameterization of *k* based on solely windspeed is flawed because several additional parameters can contribute to turbulence including turbidity, bottom-driven turbulence, water-side thermal convection, tidal currents, and fetch (Wanninkhof 1992, Abril et al., 2009, Ho et al., 2104, Andersson et al., 2017), however it is currently the best option for this system given the limited investigations of CO_2 flux and contributing factors in estuaries.

Hourly windspeed data used in calculations were retrieved from the NOAA-controlled Texas Coastal Ocean Observation Network (TCOON; https://tidesandcurrents.noaa.gov/tcoon.html). The closest station with windspeed data, Port Aransas Station, was located directly in the Aransas Ship Channel (further inshore than our monitoring location), however there were several long periods of missing data. To fill in the data gaps, wind speed data from nearby Aransas Pass Station were used, and for all subsequent gaps, data from nearby Nueces Bay Station were used. For continuous

https://doi.org/10.5194/bg-2021-19
Preprint. Discussion started: 1 February 2021
© Author(s) 2021. CC BY 4.0 License.


monitoring data, TCOON's measured hourly windspeed at each time point was used in flux calculations. For biweekly discrete samples, averaged daily windspeeds were calculated from TCOON's measured hourly windspeeds and used in flux calculations for the respective day. Monthly mean atmospheric xCO_2 data (later converted to pCO_2) were obtained from NOAA's flask sampling network of the Global Monitoring Division of the Earth System Research Laboratory at the Key Biscayne (FL, USA) station, when available (https://www.esrl.noaa.gov/gmd/dv/data/index.php?site=KEY&parameter_name=Carbon%2BDioxide). For 2019 and 2020, when xCO2 data from Key Biscayne were unavailable, monthly global average values were used (ftp://aftp.cmdl.noaa.gov/products/trends/co2/co2_mm_mlo.txt).

Factors controlling the carbonate system parameters

Thermal versus non-thermal controls on pCO_2 were investigated following Takahashi et al. (2002) over annual, seasonal, and daily time scales (Table 4). When calculating annual T/B values with discrete data, only complete years (sampling from January to December) were included. When calculating daily T/B values with continuous data, only complete days (24 hourly measurements) were included.

$$pCO_{2,thermal} = pCO_{2,mean} \times \exp[\delta \times (T_{obs} - T_{mean})] \quad (2)$$

$$pCO_{2,nonthermal} = pCO_{2,obs} \times \exp[\delta \times (T_{mean} - T_{obs})] \quad (3)$$

Where the value for δ (0.0411 $°C^{-1}$), which represents average [$\partial\, ln\, pCO_2 / \partial$ Temperature] from field observations, was taken directly from Yao and Hu (2017), T_{obs} is the observed temperature, and T_{mean} is the mean temperature over the investigated time period.

https://doi.org/10.5194/bg-2021-19
Preprint. Discussion started: 1 February 2021
© Author(s) 2021. CC BY 4.0 License.


$$T/B = \frac{\max(pCO_{2,thermal}) - \min(pCO_{2,thermal})}{\max(pCO_{2,non-thermal}) - \min(pCO_{2,non-thermal})} \quad (4)$$

Where a T/B greater than one indicates that temperature's control on pCO_2 is greater than the control from non-thermal factors (i.e. physical and biological processes) and a T/B less than one indicates that non-thermal factors' control on pCO_2 is greater than the control from temperature.

Tidal control on parameters was investigated using only the continuous monitoring data (Table 5). Hourly measurements of water level immediately offshore from the Aransas Ship Channel were obtained from NOAA's Tides and Currents Aransas Pass Station https://tidesandcurrents.noaa.gov/waterlevels.html?id=8775241&name=Aransas,%20Aransas%20Pass&state=TX. Tide data were merged with our sensor data by date and hour; given that there were gaps in available water level measurements (and no measurements prior to December 20, 2016), the usable dataset was reduced from 6088 observations to 5121 observations and fall was omitted from analyses. To examine differences between parameters during high tide and low tide, we defined high tide as tide level greater than the third quartile tide level value and low tide as a tide level less than the first quartile tide level value. The difference between high and low tide for each parameter was examined within each season (using t-tests) because of a significant interaction (based on α=0.05) between the season and high/low tide factors in a two-way ANOVA.

3. Results

3.1 Continuous monitoring results

Over the 10-month continuous monitoring period, all sensor-measured parameters showed substantial temporal variability on seasonal and diel time scales (Fig. 2, Tables 1-

https://doi.org/10.5194/bg-2021-19
Preprint. Discussion started: 1 February 2021
© Author(s) 2021. CC BY 4.0 License.


3). Mean values of sensor-measured parameters over the entire monitoring period were: temperature - 23.1°C ± 5.3°C, ranging from 9.4°C to 31.7°C; salinity - 30.8 ± 3.7, ranging from 18.3 to 38.9; pH - 8.12 ± 0.10, ranging from 7.79 to 8.45; and pCO_2 - 416 ± 60 µatm, ranging from 251 µatm to 620 µatm (Table 1). Temperature was significantly different between each season (Table 3), with the highest being summer and the lowest being winter (Table 1). Salinity was highest in the summer and lowest in the fall, and salinity differed between all seasons except from spring and winter (Tables 1 and 3). pH and pCO_2 were both significantly different between all seasons (Table 3). Winter had both the highest seasonal pH (8.19 ± 0.08) and lowest seasonal pCO_2 (365 ± 44 µatm) and summer had both the lowest seasonal pH (8.05 ± 0.06) and highest seasonal pCO_2 (463 ± 48 µatm) (Table 1, Fig. 2- 3).

Table 1. Mean and standard deviation of annual and seasonal temperature, salinity, pH, pCO_2, and CO_2 flux from continuous monitoring, discrete sampling over the continuous monitoring period, and discrete sampling over the entire sampled period. Reported annual means are seasonally weighted to account for disproportional sampling between seasons (however, reported annual standard deviation is associated with the un-weighted, arithmetic mean). CO_2 fluxes were calculated using the Jiang et al. (2008) wind speed parameterization for gas transfer velocity, and ranges of CO_2 flux that are given in brackets represent means calculated using parameterizations from Ho et al. (2006) and Raymond and Cole (2001), respectively.

Parameter		**Continuous Monitoring**		**Discrete Sampling**
	Time Period	Nov. 8 2016 – Aug 23, 2017	Nov. 8 2016 – Aug 23, 2017	May 2, 2014- Feb. 25, 2020
Temperature (°C)	**Annual**	23.1 ± 5.3	23.5 ± 5.0	24.1 ± 5.3
	Winter	17.3 ± 2.1	17.3 ± 1.1	16.2 ± 2.0
	Spring	23.8 ± 2.8	23.4 ± 2.9	22.6 ± 3.7
	Summer	29.7 ± 0.8	29.6 ± 0.5	28.7 ± 1.4
	Fall	22.5 ± 2.1	23.6 ± 0.1	25.5 ± 4.5
Salinity	**Annual**	30.8 ± 3.7	30.4 ± 3.5	30.1 ± 4.4
	Winter	30.0 ± 3.7	29.3 ± 4.6	28.9 ± 2.9
	Spring	30.2 ± 2.6	30.0 ± 1.7	28.7 ± 3.4
	Summer	33.3 ± 3.2	33.6 ± 3.2	34.6 ± 2.8
	Fall	27.6 ± 3.7	28.8 ± 0.1	28.4 ± 4.5
pH	**Annual**	8.12 ± 0.10	8.092 ± 0.078	8.079 ± 0.092
	Winter	8.19 ± 0.08	8.157 ± 0.041	8.162 ± 0.065
	Spring	8.09 ± 0.09	8.078 ± 0.056	8.077 ± 0.066

https://doi.org/10.5194/bg-2021-19
Preprint. Discussion started: 1 February 2021
© Author(s) 2021. CC BY 4.0 License.

	Summer	8.05 ± 0.06	7.999 ± 0.051	7.975 ± 0.046
	Fall	8.18 ± 0.05	8.136 ± 0.001	8.100 ± 0.071
***p*CO$_2$ (µatm)**	**Annual**	416 ± 60	400 ± 71	406 ± 100
	Winter	365 ± 44	349 ± 31	331 ± 39
	Spring	436 ± 45	413 ± 54	396 ± 67
	Summer	463 ± 48	480 ± 59	511 ± 108
	Fall	400 ± 25	357 ± 2	386 ± 62
CO$_2$ Flux (mmol m^{-2} d^{-1})	**Annual**	0.2 ± 23.7 [0.1 – (-87.6)]	-1.5 ± 9.2 [(-2.6) – (-4.5)]	(-0.8) ± 18.7 [(-0.7) – 5.3]
	Winter	(-16.9) ± 29.2 [(-14.6) – (-444.0)]	(-9.9) ± 5.2 [(-8.3) – (-16.2)]	(-13.0) ± 13.5 [(-10.6) – (-25.6)]
	Spring	7.6 ± 15.0 [6.5 – 109.0]	1.0 ± 7.1 [1.0 – 3.3]	(-6.5) ± 12.2 [(-5.5) – (-18.0)]
	Summer	10.8 ± 13.3 [9.1 – 28.9]	10.5 ± 7.8 [8.6– 16.3]	18.3 ± 19.6 [15.3 – 65.5]
	Fall	(-0.9) ± 7.7 [(-0.7) – (-44.0)]	(-7.5) [(-6.2) – (-11.4)]	(-2.3) ± 13.7 [(-1.9) – (-0.9)]

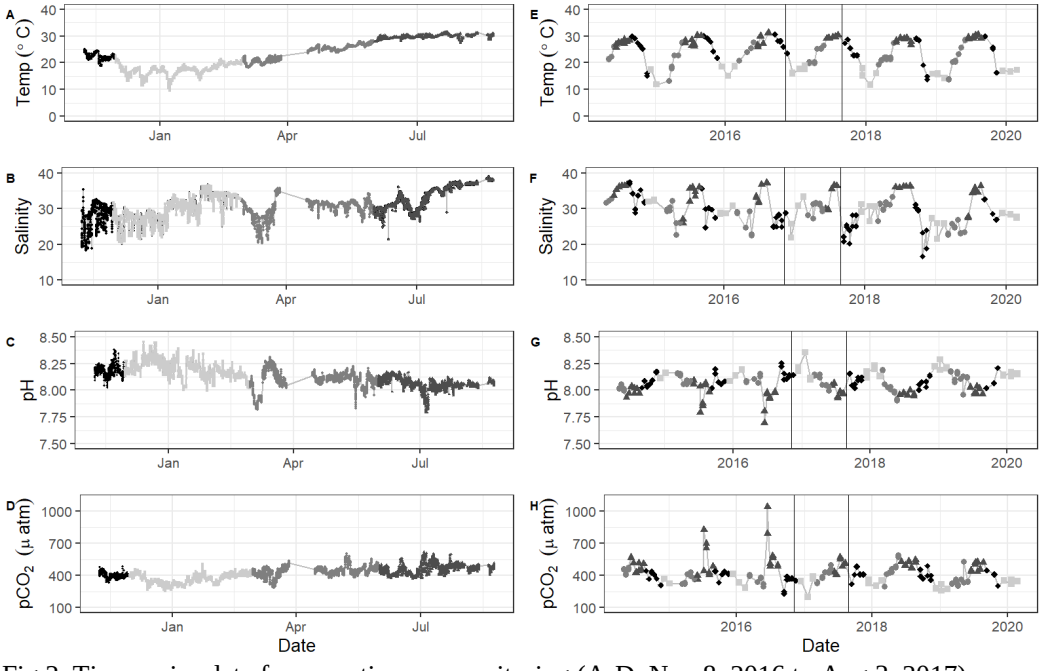

Fig 2. Time series data from continuous monitoring (A-D, Nov 8, 2016 to Aug 3, 2017) and discrete sample analysis (E-H, Nov 8, 2016 to Aug 3, 2017) at the Aransas Ship Channel. Gray scale (and shape) in the datapoints represents divisions between the four seasons. Vertical lines in (E-H) denote the time period of continuous monitoring.

https://doi.org/10.5194/bg-2021-19
Preprint. Discussion started: 1 February 2021
© Author(s) 2021. CC BY 4.0 License.

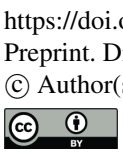

Biogeosciences
Discussions
Open Access
EGU

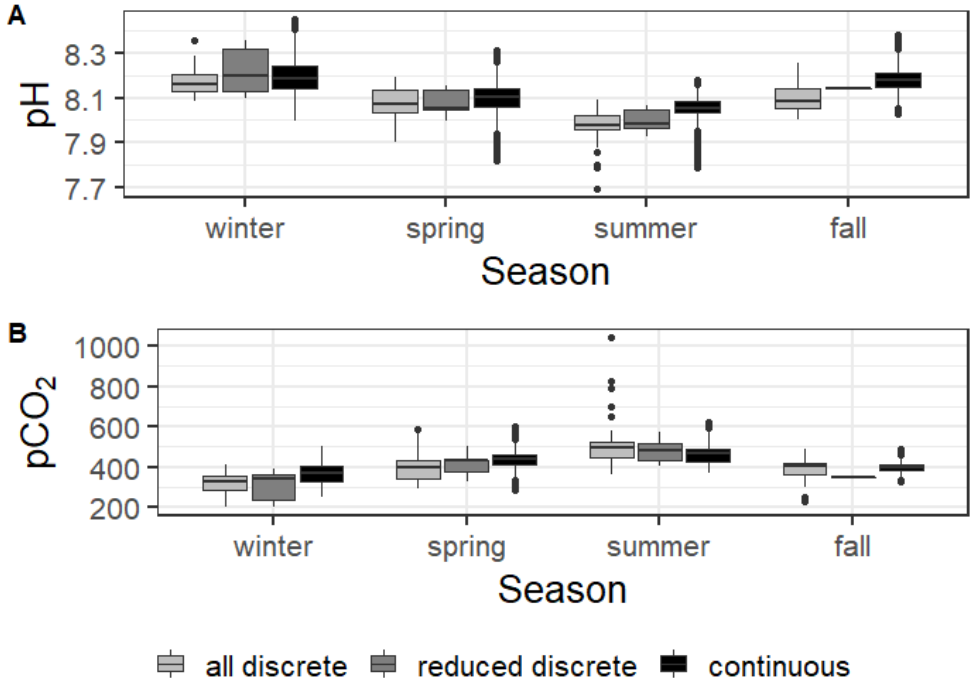

Figure 3. Boxplots of seasonal variability in pH and pCO_2 using all discrete data (May 2, 2014- Feb. 25, 2020), reduced discrete data (Nov. 8 2016 – Aug 23, 2017, to overlap with continuous monitoring), and continuous sensor data (Nov. 8 2016 – Aug 23, 2017)

Table 2. Diel variability in system parameters from continuous sensor data (Nov 8, 2016 – Aug 23, 2017). The p-values reported are from a paired-*t* test comparing the means of each day (9am-3pm LST) with the mean of the same night (9pm – 3am LST); all significant results based on α=0.05 are bolded. Diel range calculations were done using only days with the full 24 hours of hourly measurements (176 out of 262 measured) to ensure that data gaps did not influence the calculations. Reported fluxes use the Jiang et al. (2008) gas transfer velocity parameterization. Note that the Fall season had much fewer observations than other seasons because of the timing of sensor deployment.

Parameter	Time Period	Daytime Mean	Nighttime Mean	Day versus Night p-value	Mean Diel Range	Minimum Diel Range	Maximum Diel Range
Temperature (°C)	**Full Sampling Period**	23.0 ± 5.3	23.2 ± 5.4	**<0.0001**	1.3 ± 0.8	0.30	3.93
	Winter	17.2 ± 2.1	17.4 ± 2.1	0.2055	1.5 ± 0.8	0.3	3.8
	Spring	23.7 ± 2.7	23.8 ± 2.9	0.5579	1.2 ± 0.6	0.3	3.0
	Summer	29.6 ± 0.7	29.9 ± 0.8	**<0.0001**	1.0 ± 0.6	0.3	3.8
	Fall	22.0 ± 1.19	23.0 ± 1.0	**<0.0001**	1.8 ± 0.9	0.8	3.9

https://doi.org/10.5194/bg-2021-19
Preprint. Discussion started: 1 February 2021
© Author(s) 2021. CC BY 4.0 License.

Salinity	**Full Sampling Period**	30.5 ± 4.1	31.0 ± 3.3	**0.0004**	3.4 ± 2.7	0.250	15.870
	Winter	29.6 ± 4.2	30.4 ± 3.1	**0.0051**	3.8 ± 2.2	0.25	9.48
	Spring	30.1 ± 2.6	30.2 ± 2.6	0.5604	2.5 ± 2	0.4	8.17
	Summer	33.4 ± 3.2	33.1 ± 3.3	0.0550	2.0 ± 1.7	0.3	9.73
	Fall	25.9 ± 3.9	29.0 ± 3.2	**<0.0001**	7.7 ± 3.6	1.2	15.87
pH	**Full Sampling Period**	8.12 ± 0.10	8.13 ± 0.09	**<0.0001**	0.09 ± 0.05	0.02	0.28
	Winter	8.18 ± 0.08	8.20 ± 0.07	**0.0108**	0.10 ± 0.05	0.02	0.28
	Spring	8.09 ± 0.09	8.10 ± 0.08	0.3286	0.08 ± 0.03	0.03	0.18
	Summer	8.04 ± 0.06	8.07 ± 0.05	**<0.0001**	0.08 ± 0.04	0.03	0.19
	Fall	8.20 ± 0.05	8.17 ± 0.05	**0.0038**	0.12 ± 0.04	0.03	0.20
***p*CO$_2$ (µatm)**	**Full Sampling Period**	417 ± 54	416 ± 65	0.7065	58 ± 33	12.6	211.3
	Winter	374 ± 44	358 ± 43	**<0.0001**	43 ± 21	12.6	121.1
	Spring	438 ± 42	437 ± 48	0.7237	61 ± 31	20.5	152.8
	Summer	452 ± 44	471 ± 51	**0.0003**	74 ± 42	23.6	211.3
	Fall	406 ± 24	399 ± 27	0.0545	56 ± 18	22	92.2
CO$_2$ Flux (mmol m^{-2} d^{-1})	**Full Sampling Period**	0.0 ± 6.3	-1.3 ± 5.9	0.3028	34.1 ± 29.0	2.7	189.0
	Winter	-14.9 ± 8.4	-19.1 ± 7.7	0.0676	46.6 ± 38.9	2.7	189.0
	Spring	7.6 ± 5.2	7.0 ± 5.2	0.6680	27.5 ± 18.5	4.9	115.0
	Summer	9.4 ± 5.6	11.7 ± 5.2	0.1167	32.3 ± 22.9	4.5	111.0
	Fall	0.1 ± 3.8	-0.3 ± 3.5	0.7449	17.0 ± 10.2	3.9	40.1

Table 3. Tests examining differences in mean carbonate system parameters between seasons and between types of sampling (continuous monitoring with sensors Nov. 8 2016 – Aug 23, 2017, discrete sample collection and laboratory measurement during only the continuous monitoring period Nov. 8 2016 – Aug 23, 2017, and discrete sample collection and laboratory measurement during the entire sampling period May 2, 2014-Feb. 25, 2020). For both the two-way ANOVA and associated one-way ANOVAs, p-values are listed. All significant results based on α=0.05 are bolded, and the F statistic is in parentheses. Since all two-way ANOVAs had a significant interaction between factors, individual one-way ANOVAs were conducted for each level of the other factor. Following significant one-way ANOVAs, multiple comparisons using the Westfall adjustment (Westfall, 1997) were conducted; individual comparisons with significantly different means (based on α=0.05) are listed as unequal beneath the one-way ANOVA results (All≠ indicates that every individual comparison between levels had significantly different means. W = winter, Sp = spring, Su = summer, F = fall; C = continuous sensor data, D = discrete sample data over the entire discrete monitoring period, D$_C$ = Discrete sample data during only the period of continuous monitoring).

Parameter	**Two-way ANOVA**			**One-way ANOVA and post-hoc multiple comparison results for differences between types of sampling**				**One-way ANOVA and post-hoc multiple comparison results for difference between seasons**		
	Interaction	Season	Sampling type	winter	spring	summer	fall	Continuous	Discrete (Continuous Period)	Discrete (Entire Period)

https://doi.org/10.5194/bg-2021-19
Preprint. Discussion started: 1 February 2021
© Author(s) 2021. CC BY 4.0 License.

Temp (°C)	**<0.0001** (15.8)	**<0.0001** (12369.7)	0.7346 (0.3)	0.0710 (2.6)	0.1052 (2.3)	**<0.0001** (19.6) D≠C	**<0.0001** (61.4) D≠C	**<0.0001** (12559) All≠	**<0.0001** (22.8) W≠Su; W≠Sp; W≠F; Su≠Sp; Su≠F	**<0.0001** (58.2) All≠
Salinity	**0.0141** (2.7)	**<0.0001** (598.7)	0.6509 (0.4)	0.1716 (1.8)	**0.0013** (6.7) D≠C	0.1921 (1.7)	0.7007 (0.4)	**<0.0001** (580.0) W≠Su; W≠F; Su≠Sp; Su≠F; Sp≠F	0.2516 (1.6)	**<0.0001** (17.5) W≠Su; Su≠Sp; Su≠F
pH	**0.0013** (3.7)	**<0.0001** (1412.3)	**<0.0001** (24.0)	0.4026 (0.9)	0.9238 (0.1)	**<0.0001** (24.1 D≠C **C≠D$_C$**	**<0.0001** (33.2) D≠C	**<0.0001** (1381.2) All≠	**0.0152** (5.7) W≠Su	**<0.0001** (35.3) W≠Su; W≠Sp; W≠F; Su≠Sp; Su≠F
***p*CO$_2$ (µatm)**	**<0.0001** (10.4)	**<0.0001** (1747.3)	**0.0147** (4.2)	**0.0018** (6.4) D≠C	**<0.0001** (17.4) D≠C	**0.0002** (8.4) D≠C	0.0398 (3.2) **All=**	**<0.0001** (1737.6) All≠	**0.0407** (4.0) W≠Su	**<0.0001** (8.4) W≠Su; W≠Sp; W≠F; Su≠Sp; Su≠F
CO$_2$ Flux (mmol m^{-2} d^{-1})	**0.0144** (2.6)	**<0.0001** (738.1)	0.6739 (0.4)	0.9140 (0.1)	**<0.0001** (11.8) D≠C	**0.0214** (3.9) D≠C	0.5849 (0.5)	**<0.0001** (725.9) All≠	**0.0299** (4.5) W≠Su	**<0.0001** (19.2) W≠Su; W≠F; Su≠Sp; Su≠F

There was substantial diel variability in parameters (Table 2, Fig. 4). Over the 10-month in-situ monitoring period, temperature had a mean diel range (daily maximum minus daily minimum) of 1.3 ± 0.8°C (Table 2). Daytime and nighttime temperature differed significantly during the summer and fall months, with higher temperatures at night for both seasons (Table 2). The mean diel range of salinity was 3.4 ± 2.7 (Table 2). Daytime and nighttime salinity differed significantly during the winter and fall months, with higher salinities at night for both seasons. The mean diel range of pH was 0.09 ±

https://doi.org/10.5194/bg-2021-19
Preprint. Discussion started: 1 February 2021
© Author(s) 2021. CC BY 4.0 License.

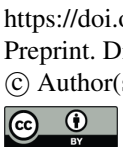

0.05 (Table 2). Daytime and nighttime pH differed significantly during the winter, summer, and fall months; nighttime pH was significantly higher than that of the daytime during the summer and winter months, and daytime pH was significantly higher during the fall (Table 2, Fig. 4). The mean diel range of pCO_2 was 58 ± 33 µatm (Table 2, Fig. 4). Daytime and nighttime pCO_2 differed significantly during the winter and summer months; nighttime pCO_2 was significantly higher than that of the daytime during the summer and daytime pCO_2 was significantly higher during the winter (Table 2, Fig. 4).

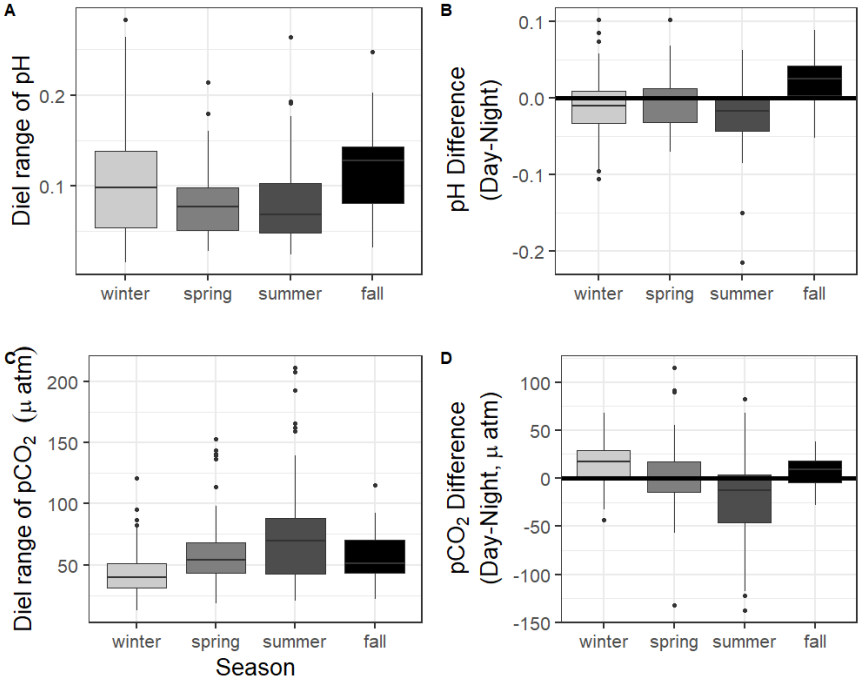

Figure 4. Boxplots showing the diel range (maximum minus minimum) and difference in daily parameter mean daytime minus nighttime measurements for pH and pCO_2 from continuous sensor data.

The seasonally weighted mean CO_2 flux calculated from sensor data across the entire monitoring period was 0.2 ± 23.7 mmol m^{-2} d^{-1} (Table 1). Mean CO_2 flux differed by season (Table 3). Winter and fall both had net negative CO_2 flux (winter was most

https://doi.org/10.5194/bg-2021-19
Preprint. Discussion started: 1 February 2021
© Author(s) 2021. CC BY 4.0 License.

negative), and summer and spring both had a net positive CO_2 flux (summer was most positive) (Table 1, Fig. 5). CO_2 flux also fluctuated on a daily scale, with the mean diel range (daily maximum – minimum) over the entire monitoring period being 34.1 ± 29.0 mmol m^{-2} d^{-1} (Table 2). However, there was not a significant difference in CO_2 flux calculated for daytime versus nighttime hours for the entire monitoring period or any individual season based on α=0.05 (paired t-test, Table 2).

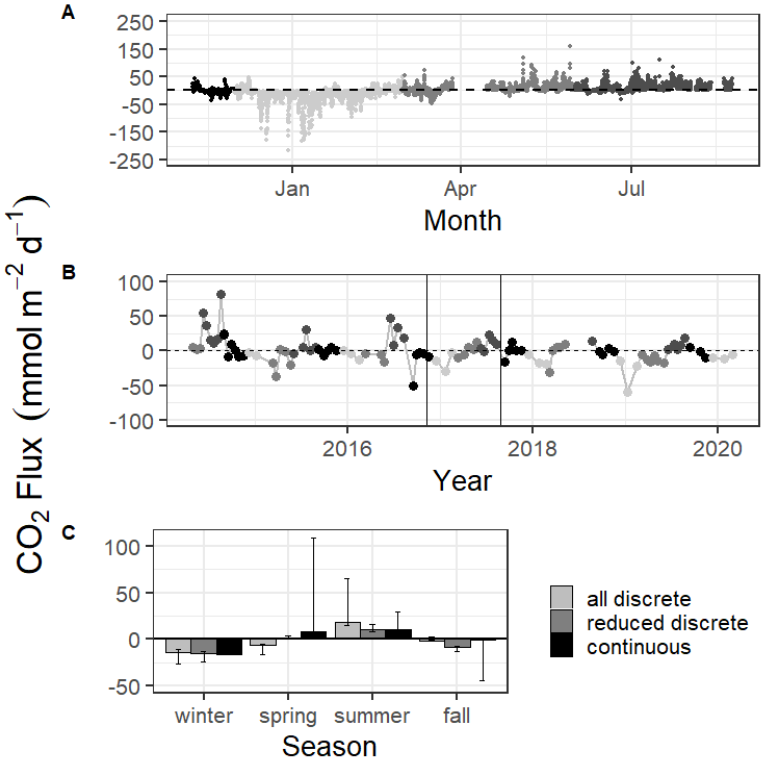

Figure 5. CO_2 flux calculated over the sampling periods from continuous (A) and discrete (B) data using the Jiang et al. (2008) wind speed parameterization. Gray scale in (A) and (B) denote different seasons. Vertical lines in (B) denote the time period of continuous monitoring. (C) shows the seasonal mean CO_2 flux calculated using the Jiang et al. (2008) gas transfer velocity parameterization and error bars representing mean CO_2 flux calculation using Ho and Raymond and Cole windspeed parameterizations. The different color bars within each season represent all discrete data (May 2, 2014- Feb. 25, 2020), reduced discrete data (Nov. 8 2016 – Aug 23, 2017, to overlap with continuous monitoring), and continuous sensor data (Nov. 8 2016 – Aug 23, 2017).

https://doi.org/10.5194/bg-2021-19
Preprint. Discussion started: 1 February 2021
© Author(s) 2021. CC BY 4.0 License.

The relative influence of thermal and nonthermal factors (T/B) in controlling pCO_2 varied over different time scales (Table 4, Fig. 6). T/B calculated from sensor data for the entire period was 0.98, indicating that the magnitude of control of non-thermal processes on pCO_2 was slightly greater than that of temperature. Within seasons, T/B calculated from sensor data ranged from 0.51 in the winter to 0.69 in the spring, showing that non-thermal processes exert more control on pCO_2 within each individual season (Table 4). On a daily scale, only 11 of the 178 days with measurements for all 24 hours had temperature control of pCO_2 exceeding the non-thermal control (Table 4, Fig. 6).

Table 4. Thermal versus non-thermal control on pCO_2 (Takahashi et al. 2002) over different time scales using both continuous sensor data and discrete sample data (indicated as Sampling Type C and D, respectively). If more than one segment of time is being considered (n>1), ΔpCO_2 values are the mean ± standard deviation of all segments, the T/B values are the minimum and maximum T/B, and the number out of n with T/B>1 (indicating greater control of pCO_2 by temperature than other processes) is recorded. The summary of annual T/B values from discrete data includes only 2015-2019 (n=5 years; 2014 and 2020 were omitted since monitoring did not occur throughout the entire year). Daily values from continuous data were only reported for those days with all 24 measurements.

Time Period / Scale	Sampling type	n	$\Delta pCO_{2,\,thermal}$ (µatm)	$\Delta pCO_{2,\,nonthermal}$ (µatm)	T/B	Number out of n with T/B >1
Full Monitoring Period (May 2, 2014- Feb. 25, 2020)	D	1	301.9	537.8	0.56	
Annual	D	5	259.3 ± 16.0	319.1 ± 130.9	0.48 – 1.17	2/5
Continuous Monitoring Period	C	1	355.0	360.7	0.98	
(Nov 2016 – August 2017)	D	1	236.3	229.9	1.03	
Winter	C	1	168.2	328.4	0.51	
	D	6	42.2 ± 23.4	101.7 ± 78.7	0.20 – 4.90	1/6
Spring	C	1	171.4	246.9	0.69	
	D	6	142.3 ± 53.7	147.8 ± 67.3	0.59 – 2.42	2/6
Summer	C	1	100.2	179.9	0.56	
	D	6	46.9 ± 26.6	176.9 ± 108.3	0.21 – 0.35	0/6
Fall	C	1	105.9	181.6	0.58	
	D	6	179.8 ± 59.5	176.6 ± 78.1	0.59 – 3.06	2/6
Daily	C	178	21.8 ± 11.8	63.8 ± 30.3	0.05 – 1.68	11/178

https://doi.org/10.5194/bg-2021-19
Preprint. Discussion started: 1 February 2021
© Author(s) 2021. CC BY 4.0 License.

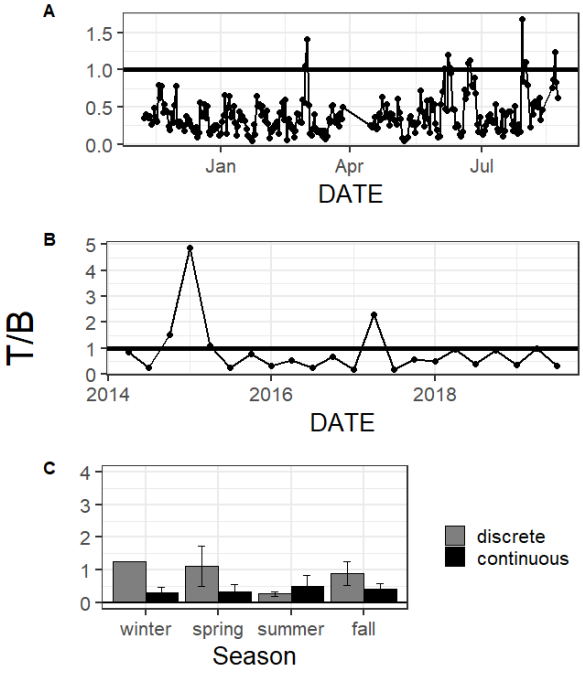

Figure 6. T/B (thermal pCO_2/ non-thermal pCO_2) calculated for each day from continuous (A) and each season from discrete (B) data. Bar graphs showing the seasonal mean and standard deviation of T/B from both discrete and continuous data (C).

Tidal fluctuations had a significant effect on carbonate system parameters (Table 5). Both temperature and salinity were higher at low tide during the winter and summer months and higher at high tide during the spring. pH was higher at high tide during the winter and summer and higher at low tide during the spring, and pCO_2 was higher during low tide during winter, spring, and summer (Table 5). CO_2 flux also varied with tidal fluctuations. CO_2 flux was higher in the low tide condition for all season with tide data; the location was less of a CO_2 sink during low tide conditions in the winter and more of a CO_2 source during low tide conditions in the spring and summer.

Table 5. Differences in temperature, salinity and mean carbonate system parameters from continuous sensor data between high tide and low tide. High tide was defined as a tide level greater than Q3 and low tide was defined as a tide level less than Q1. Seasons were examined separately with t-tests because of a significant interaction (based on α=0.05)

https://doi.org/10.5194/bg-2021-19
Preprint. Discussion started: 1 February 2021
© Author(s) 2021. CC BY 4.0 License.


between the season and high/low tide factors in a two-way ANOVA. Fall was omitted from the analysis because tide data was only available at the location beginning December 20, 2016.

Parameter	Season	High Tide Mean	Low Tide Mean	Difference between tide levels, t-test p-value
Temperature (°C)	Winter	16.7 ± 1.7	17.6 ± 2.0	**<0.0001**
	Spring	24.4 ± 2.7	23.6 ± 2.7	**<0.0001**
	Summer	29.3 ± 0.5	30.1 ± 0.7	**<0.0001**
Salinity	Winter	30.2 ± 2.5	31.3 ± 2.9	**<0.0001**
	Spring	30.4 ± 1.9	30.0 ± 2.7	**0.0071**
	Summer	30.5 ± 2.4	34.5 ± 3.0	**<0.0001**
pH	Winter	8.20 ± 0.08	8.15 ± 0.06	**<0.0001**
	Spring	8.07 ± 0.09	8.10 ± 0.07	**<0.0001**
	Summer	8.08 ± 0.04	8.04 ± 0.06	**<0.0001**
pCO_2 (µatm)	Winter	331 ± 40	378 ± 42	**<0.0001**
	Spring	435 ± 33	443 ± 50	**0.0154**
	Summer	419 ± 30	482 ± 48	**<0.0001**
CO_2 Flux (mmol m^{-2} d^{-1})	Winter	-33.0 ± 38.1	-11.7 ± 21.8	**<0.0001**
	Spring	7.4 ± 14.0	8.7 ± 14.8	**0.2248**
	Summer	1.8 ± 6.3	16.0 ± 14.5	**<0.0001**

3.2 Discrete sampling results

All results reported here are for the entire 5+ years of monitoring; the subset of discrete sample data that overlaps with the continuous monitoring period will be addressed only in the discussion for method comparisons. All reported discrete sampling parameters showed substantial temporal variability over the 5+ years of monitoring (Fig. 2E-H). The mean temperature was 24.1 ± 5.3°C, ranging from 11.8 – 31.2°C; the mean salinity was 30.1 ± 4.4, ranging from 16.7 – 37.5; the mean pH was 8.079 ± 0.092, ranging from 7.693 to 8.354; and the mean pCO_2 was 406 ± 100 µatm, ranging from 199 to 1043 (Table 1). These parameters all experienced significant seasonal variability (Tables 1 and 3). Temperature was significantly different between each season, highest in summer and lowest in winter (Tables 1 and 3). Salinity was highest during the summer months and was not significantly different between other seasons (Tables 1 and 3). pH and pCO_2 were both significantly different between all seasons with the exception of

https://doi.org/10.5194/bg-2021-19
Preprint. Discussion started: 1 February 2021
© Author(s) 2021. CC BY 4.0 License.


spring and fall (Table 3). Winter had both the highest seasonal pH (8.162 ± 0.065) and lowest seasonal pCO_2 (331 ± 39 µatm), and summer had both the lowest seasonal pH (7.975 ± 0.046) and highest seasonal pCO_2 (511 ± 108) (Tables 1 and 3, Fig. 3).

Average annual CO_2 flux calculated with discrete sample data was slightly negative (-0.9± 18.7 mmol m^{-2} d^{-1}, Table 1). CO_2 flux varied greatly by season. Summer, the only season with a net positive CO_2 flux over the 5+ year period, had significantly higher flux than all other seasons; winter had the lowest calculated flux, but it was not significantly different from spring (Tables 1 and 3).

As with the continuous data, T/B calculated from the discrete data varied over different time scales (Table 4, Fig. 6). For the entire period, T/B was 0.56, indicating that non-thermal processes exerted more control than temperature on pCO_2. The annual T/B varied from 0.48 to 1.17, with two of the five sampled years having T/B greater than one (i.e. more thermal influence). While the majority of individual seasons that were sampled experienced stronger non-thermal control on pCO_2 (T/B <1), the only season that never experienced stronger thermal control was summer, with summer T/B values ranging from 0.21 – 0.35 for the 6 sampled years (Table 4).

Discussion

4.1 Factors controlling temporal variability in carbonate system parameters

4.1.1 Thermal versus non-thermal control of pCO_2

Substantial variability in the carbonate system was observed at the study site over multiple time scales including diel, seasonal, and interannual. Many physical and biological factors (e.g., temperature, currents, tides, wind speed, net ecosystem metabolism, etc.) can exert control on pCO_2 and subsequently exert control on other

https://doi.org/10.5194/bg-2021-19
Preprint. Discussion started: 1 February 2021
© Author(s) 2021. CC BY 4.0 License.


carbonate system parameters. Using the thermal versus non-thermal analysis of control on pCO_2 from Takahashi et al. (2002), we were able to determine that non-thermal processes generally exert more control on the pCO_2 in the Aransas Ship Channel relative to temperature over multiple time scales (Table 4, T/B<1). Only five of 24 seasons (one winter, two spring, and two fall) throughout the years of discrete sampling had greater variability in pCO_2 attributed to temperature ($\Delta pCO_{2,\ thermal}$) than other processes ($\Delta pCO_{2,\ nonthermal}$) (Table 4). The magnitude of pCO_2 variation attributed to non-thermal processes varied greatly over multiple time scales (i.e. $\Delta pCO_{2,\ nonthermal}$ had large standard deviations, Table 4). For example, in 2016 pCO_2 had the strongest non-thermal control of any year, with a $\Delta pCO_{2,\ nonthermal}$ of 538 µatm, while 2019 had the weakest control from non-thermal processes of any year, with a $\Delta pCO_{2,\ nonthermal}$ of 208. Conversely, the magnitude of pCO_2 variation attributed to temperature was consistent across time scales. For example, in 2015 pCO_2 had the strongest thermal control of any year, with a $\Delta pCO_{2,\ thermal}$ of 276 µatm, while 2019 had the weakest thermal control of any year, with a $\Delta pCO_{2,\ thermal}$ of 243 µatm.

The difference in T/B between sampling methods is relatively small over the 10-month sensor deployment period (Table 4). Each method suggested temperature and nonthermal processes exert a relatively similar control on pCO_2, but continuous monitoring demonstrated a greater magnitude of fluctuation resulting from both temperature and non-thermal processes (i.e. greater $\Delta pCO_{2,\ thermal}$ and $\Delta pCO_{2,\ nonthermal}$). Over shorter time scales, like individual seasons, the calculated T/B did not align well between sampling methods. The T/B (calculated using only data from Nov 2016 – August 2017) for discrete versus continuous sampling was respectively 0.17 versus 0.51

https://doi.org/10.5194/bg-2021-19
Preprint. Discussion started: 1 February 2021
© Author(s) 2021. CC BY 4.0 License.


for winter, 2.37 versus 0.69 for spring, and 0.20 versus 0.56 for summer (Table 4, Fall was omitted since there was only one discrete sampling event during the fall of the continuous monitoring period). Sampling bias due to the small number of within-season sampling events for the discrete monitoring likely resulted in this difference. From both continuous and discrete data, summers always had stronger control exerted on pCO_2 from nonthermal processes than temperature. While temperatures were high during the summer months, the within-season variability in temperature was the lowest (Table 1); less of a temperature swing resulted in less thermal control on the system. Conversely, spring and fall seasons, which experienced the greatest temperature swings (Table 1), had greater relative temperature control exerted on pCO_2 (Table 4). The differences in $\Delta pCO_{2,\,thermal}$ and $\Delta pCO_{2,\,nonthermal}$ between monitoring methods illustrate that there is information that is missed when only sampling bimonthly/monthly and during the daytime. Generally, both $\Delta pCO_{2,\,thermal}$ and $\Delta pCO_{2,\,nonthermal}$ are higher when calculated from sensors than discrete sampling, indicating that the extremes are generally not captured by the discrete sampling and sensor data would provide a better understanding of system controls.

The relative importance of thermal versus non-thermal controls may be modulated by tide level. The influence of tides can be removed from the calculated non-thermal pCO_2 term, leaving only biological processes and other physical controls in the non-thermal term, by examining periods of high tide and low tide separately. Using our sensor data and the same water level data used for the tide analysis, we found that T/B is higher during the high tide condition within each season. T/B for high tide and low tide, respectively, was 0.60 and 0.52 for winter, 0.84 and 0.66 for spring, and 0.62 and 0.58 for

https://doi.org/10.5194/bg-2021-19
Preprint. Discussion started: 1 February 2021
© Author(s) 2021. CC BY 4.0 License.


summer. The higher control exerted by nonthermal processes during low tide seems intuitive given that there is less volume of water for the end products of biological processes to build up in. The difference in T/B between high tide and low tide conditions was greatest in the spring, likely due to a combination of elevated spring-time productivity and larger tidal ranges in the spring.

Using data from the first year of our discrete sampling (May 2014 – April 2015), Yao and Hu (2017) reported that the Aransas Ship Channel T/B was 1.53 during drought and 1.79 during a period of flooding, both of which are significantly higher than what we found over most timescales (the exception being certain individual seasons, mostly during that first year of sampling, Table 4, Fig. 6B). Yao and Hu (2017) also found that locations in the upper estuary experienced lower T/B during flooding conditions than drought conditions, but the opposite was found for the Aransas Ship Channel location, where the flooding conditions had higher T/B. It is likely that the high T/B calculated by Yao and Hu (2017) was a result of the drought condition at the beginning of their sampling; given the long residence time of MAE, the Aransas Ship Channel may not have experienced the influence of the freshwater inflow by the end of the Yao and Hu (2017) study. Once the freshwater reached the Aransas Ship Channel location, it would likely experience a reduced T/B as did the upper parts of the system. Since then, there has not been another significant drought in the system, so it seems as though the non-thermal controls on pCO_2 are more important at this location under normal freshwater inflow conditions.

https://doi.org/10.5194/bg-2021-19
Preprint. Discussion started: 1 February 2021
© Author(s) 2021. CC BY 4.0 License.


534 *4.1.2 Investigating controls on the carbonate system using relationships between*
535 *carbonate system parameters and other environmental parameters*

536 We further investigated controls on the carbonate system using tide and
537 windspeed data (obtained from NOAA's Aransas Pass station at
538 https://tidesandcurrents.noaa.gov/) and dissolved oxygen, PAR, turbidity, and chlorophyll
539 fluorescence data (obtained from the MANERR at
540 https://missionaransas.org/science/download-data) along with our continuous and discrete
541 data. All investigations of relationships between environmental parameters discussed
542 below included only the observations with no significant water column stratification
543 (defined as a salinity difference of less than 3 between surface water from our YSI and
544 bottom water (>5 m) from the MANERR's YSI). This omission of stratified water was
545 intended to omit instances of substantial differences in chemical parameters between the
546 surface and bottom water since all MANERR environmental data used in our analysis
547 were measured at depth while our sensors measured surface water. Omitting stratified
548 water reduced our continuous dataset from 6088 to 5524 observations, and omitting
549 observations where there were no MANERR data to determine stratification further
550 reduced the dataset to 4112 observations. Similarly, removing instances of stratification
551 reduced discrete sample data from 104 to 89 surface water observations.

552 To extend upon the above discussion of thermal versus non-thermal controls on
553 pCO_2, the extent of thermal control on both pH and pCO_2 can be investigated based on
554 relationships between parameters. There is a strong negative correlation between pH and
555 temperature and a strong positive correlation between pCO_2 and temperature (Table 6,
556 Fig. 7). The direction of these relationships (sign of the correlation coefficient) at the

https://doi.org/10.5194/bg-2021-19
Preprint. Discussion started: 1 February 2021
© Author(s) 2021. CC BY 4.0 License.

Aransas Ship Channel was the same as in open ocean waters despite these relationships not being consistent across different estuarine environments (N. Rosenau, personal communications). The strong correlations with temperature support our findings that thermal controls on pCO_2 can be important over multiple time scales. Significantly warmer water temperatures were observed during the nighttime in both summer and fall (Table 2, Fig. 8), indicating that temperature could exert a slight control on the carbonate system over a diel time scale. More substantial temperature swings between seasons indicate that temperature is more important over seasonal time scales (Table 1). In addition to direct thermal control at our site, the strong correlations with temperature are likely derived from changes in net community metabolism associated with temperature (Caffrey, 2004). For example, the strong negative correlation between nonthermal pCO_2 and temperature (Table 6) is likely indicative of enhanced primary productivity in warmer waters.

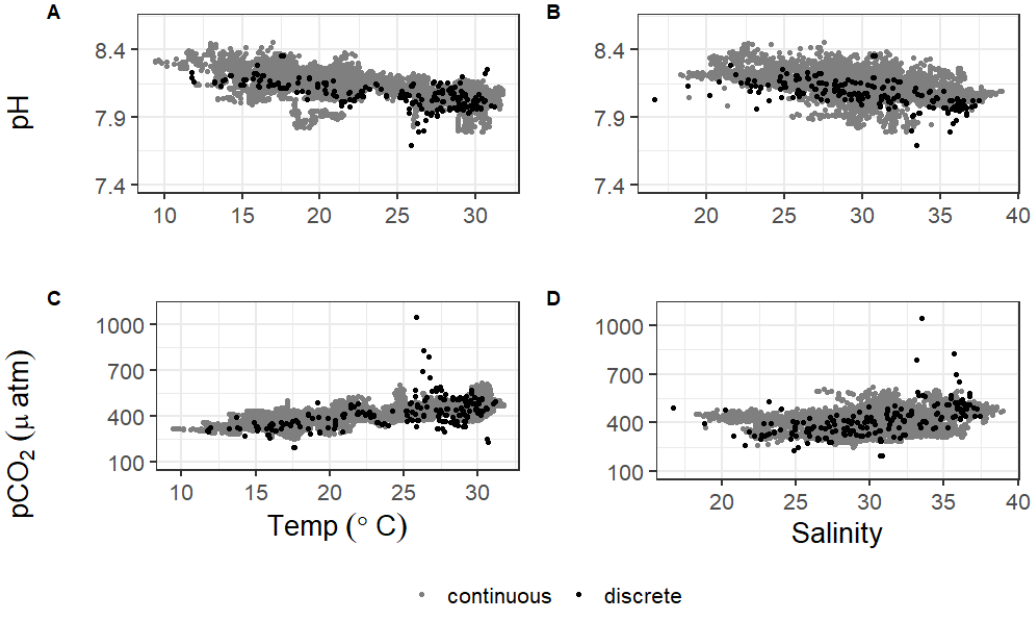

https://doi.org/10.5194/bg-2021-19
Preprint. Discussion started: 1 February 2021
© Author(s) 2021. CC BY 4.0 License.

571 Figure 7. Correlations of pH and pCO_2 with temperature and salinity from continuous
572 sensor data (gray) and all discrete data (black).
573

574 Table 6. Pearson correlation coefficients between surface water carbonate system
575 parameters and other water quality and environmental parameters for both continuous
576 sensor data and discrete sample data (entire sampling period). Only observations without
577 significant stratification in the water column were included in these analyses. Parameter
578 pairs with a significant correlation based on α=0.05 have a correlation coefficient
579 reported. Asterixis are used to indicate the level of significance of the correlation, *
580 $p<0.05$, ** $p<0.01$, *** $p<0.0001$. The correlation coefficient is listed as 0 if the
581 relationship was not significant. N/A is listed when the analysis was omitted because the
582 environmental parameter did not have observations corresponding to the date and time of
583 at least half of our discrete sample measurements (45 observations).

	pH		***p*CO₂**		***p*CO₂, nonthermal**	
	Continuous	**Discrete**	**Continuous**	**Discrete**	**Continuous**	**Discrete**
Temperature (°C)	-0.55 ***	-0.59 ***	0.75 ***	0.53 ***	-0.73 ***	-0.45 ***
Salinity	-0.47 ***	-0.74 ***	0.53 ***	0.69 ***	-0.28 ***	0.35 **
Wind Speed (m s^{-1})	-0.04 **	N/A	0.15 ***	N/A	0	N/A
Dissolved Oxygen (mg L^{-1})	0.55 ***	0	-0.81 ***	0	0.45 ***	0
Tide Level (m)	0	0	-0.15 ***	0	-0.15 ***	-0.55 **
Turbidity	-0.08 ***	N/A	-0.14 ***	N/A	-0.28 ***	N/A
Fluor. Chlorophyll	0.12 ***	N/A	-0.22 ***	N/A	0.34 ***	N/A

584
585 Though annual average pCO_2 and CO_2 flux are higher in the upper estuary and
586 lower offshore than at our study site, the same seasonal pattern of elevated pCO_2 and
587 positive CO_2 flux in the summer and depressed pCO_2 and negative CO_2 flux during the
588 winter observed at our site has also been observed throughout the entire MAE and in the
589 open Gulf of Mexico (Hu et al., 2018; Yao and Hu, 2017). Seasonal fluctuations in pH
590 and pCO_2 are low at our study site relative to other systems that have been studied to date
591 (Carstensen et al., 2018; Yao and Hu, 2017), which may be in part due to the relatively
592 small seasonal temperature changes (Table 1) in this warm, semiarid environment.
593 Despite substantial seasonal thermal control at our site, simple linear regressions indicate
594 that temperature had substantially higher explanatory value for pH and pCO_2 in offshore
595 GOM waters (R^2 = 0.81 and 0.78, respectively (Hu et al., 2018)) than at our site (R^2 =

https://doi.org/10.5194/bg-2021-19
Preprint. Discussion started: 1 February 2021
© Author(s) 2021. CC BY 4.0 License.


596 0.30 and 0.52, respectively, for sensor data and R^2 = 0.38 and 0.25, respectively, for
597 discrete data).

598 Other physical factors that may exert control on the carbonate system (including
599 windspeed, salinity, tide level, and turbidity) can also be investigated through parameter
600 relationships. We investigated wind speed as a possible control on the carbonate system
601 to gain insight into the effect of wind-driven CO_2 fluxes on the inventory of CO_2 in the
602 water column (and subsequent impacts to the entire carbonate system). The Texas coast
603 has relatively high wind speeds, with the mean wind speed observed during our
604 continuous monitoring period being 5.8 m s^{-1}. While this results in relatively high
605 calculated CO_2 fluxes (Fig. 5), the seasonal relationship between pCO_2 and windspeed
606 does not support a change in inventory with higher winds. Linear regression analysis
607 within each season reveals that winter, spring, and fall all experience increases in pCO_2
608 with increasing wind, while there is not a significant relationship in summer. Since spring
609 and summer both have a mean estuarine pCO_2 greater than atmospheric level (and
610 positive CO_2 flux, Table 1) a negative relationship between windspeed and pCO_2 would
611 be necessary to support this hypothesis.

612 Previous studies have indicated that freshwater inflow may exert a primary
613 control on the carbonate system in the estuaries of the northwestern GOM (Hu et al.,
614 2015; Yao et al., 2020; Yao and Hu, 2017). Increased freshwater inflow resulting from
615 storms has also been shown to increase community respiration, which would
616 subsequently increase pCO_2, in the upper reaches of the MAE (Bruesewitz et al., 2013).
617 MAE is also known to experience large swings in the chemistry of its freshwater inputs,
618 with relatively high levels of dissolved inorganic carbon and total alkalinity during base

https://doi.org/10.5194/bg-2021-19
Preprint. Discussion started: 1 February 2021
© Author(s) 2021. CC BY 4.0 License.


flows but much lower levels due to dilution during intense flooding (Yao et al., 2020). Given the location of our sampling in the lower portion of the estuary and the long residence time in the system, we will not directly address freshwater inflows as a controlling factor, but the influence of freshwater inflow may be evident in the response of the system to changes in salinity. Carbonate system variability is much lower at our study site than it is in the more upper reaches of MAE, likely due to the lesser influence of freshwater inflow and its associated changes in biological activity at the Aransas Ship Channel (Yao and Hu, 2017). Salinity from both sensor and discrete monitoring was strongly correlated with pH and pCO_2, with correlation coefficients nearing (continuous) or surpassing (discrete) that of the correlations with temperature (Fig. 7; Table 6). Periods of lower salinity had higher pH and lower pCO_2, likely due to enhanced freshwater influence and subsequent elevated primary productivity at the study site. Fluctuating salinity at the Aransas Ship Channel may also result from direct precipitation, stratification, and tidal fluctuations. Based on the simple linear regression of salinity with tide level, there is a significant ($p<0.0001$) relationship between tide level and salinity, but the amount of variability in salinity that tides can explain (based on model R^2) is only about 2%.

Tidal fluctuations were clearly important to carbonate system variability at the Aransas Ship Channel (Table 5). While the northwestern GOM estuaries are generally microtidal, the constricted tidal inlets such as the Aransas Ship Channel may experience relatively large tidal fluctuations. The water level data used in this analysis came from a location directly offshore from our study site, and water level had a range of 1.30 m (maximum – minimum recorded water level) over the 10-month continuous monitoring

https://doi.org/10.5194/bg-2021-19
Preprint. Discussion started: 1 February 2021
© Author(s) 2021. CC BY 4.0 License.


period. Mean water level varied between all seasons; mean spring (highest) water levels were on average 0.08 m higher than winter (lowest) water levels (ANOVA $p<0.0001$, fall was not considered because of a lack of water level data). Tidal influence on pH was less clear. Data from continuous monitoring did not show a significant correlation between pH and tide level across the entire monitoring period (Table 6). Significant differences in mean pH between tide levels were recorded during each season; pH was higher at high tide (corresponding with the lower pCO_2) during the winter and summer, but pH was lower at high tide (conflicting with the lower pCO_2) in the spring (Table 5). This separation between water level correlation with pH and pCO_2 suggests that different controlling factors of the carbonate system may not be exerted equally on both pCO_2 and over different timescales. Similar to pH, both temperature and salinity experienced seasonally dependent reversals in their difference between tide levels during the spring; each were higher at low tide during winter and summer and higher at high tide during spring (Table 5). Given the negative relationship of both temperature and salinity with pH, it is likely these parameters became important controls on pH in the spring.

To help examine controls on the carbonate system on a diel time scale, we used loess models (locally weighted polynomial regression) to identify changes in diel patterns over the course of our monitoring period (Fig. 8). Both tidal and biological controls on the carbonate system can operate on a diel time scale. The GOM is one of the few places in the world that experiences diurnal tides (Seim et al., 1987; Thurman, 1994), so theoretically, the fluctuations in pCO_2 associated with tides may align to either amplify or reduce/reverse the fluctuations that would result from diel variability in net community metabolism. The mean daily tidal fluctuation during our continuous monitoring period

https://doi.org/10.5194/bg-2021-19
Preprint. Discussion started: 1 February 2021
© Author(s) 2021. CC BY 4.0 License.

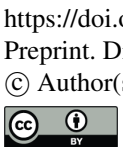

665 was 0.39 m ± 0.13 m, which did not significantly differ between seasons (ANOVA
666 p=0.739). However, diel patterns in tidal fluctuations exhibited a strong seasonal pattern
667 during the continuous monitoring period, with spring and summer having higher tide
668 level during the daytime and winter having higher tide level during the nighttime (Fig. 8).
669 This same seasonal pattern in diel tidal fluctuations is exhibited from Dec 20, 2016 (when
670 the tide data is first available) through the rest of our discrete monitoring period (Feb 25,
671 2020), indicating that tidal control on diel variability of carbonate system parameters was
672 likely consistent throughout this time period.

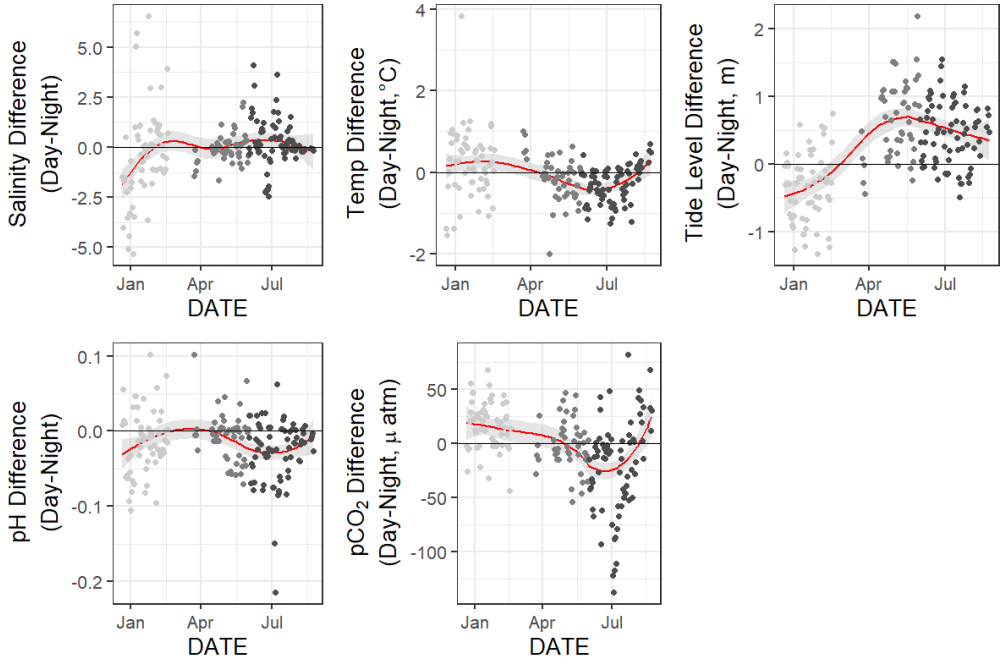

673
674 Figure 8. Loess models (red line) and their confidence intervals (gray band around red
675 line) showing the difference in daily parameter mean daytime minus nighttime
676 measurements. The gray scale of the data points represents the four seasons over which
677 data were collected.
678

679 Based on diel tidal fluctuations at this site, tidal control should amplify the
680 biological control signal (nighttime pCO_2 > daytime pCO_2) during spring and summer

https://doi.org/10.5194/bg-2021-19
Preprint. Discussion started: 1 February 2021
© Author(s) 2021. CC BY 4.0 License.


and reduce or reverse the biological control signal during the winter. This was supported by our pCO_2 data, which showed nighttime pCO_2 significantly greater than daytime pCO_2 in the summer (Table 2). The full reversal of the biological signal in the winter (Table 2, nighttime pCO_2 < daytime pCO_2) indicated that biological activity was not the strongest controlling factor on the diel time scale and was likely exceeded by tidal control. Winter also had higher daytime temperature (Table 3), which could also contribute to the higher daytime pCO_2, while summer diel temperature and tides would act to amplify the biological signal.

Again, the diel variability in pH did not mirror pCO_2 as would be expected. The loess models show that daily variability in pH closely mirrors that of temperature while the daily variability in pCO_2 much closer reflects the tide level (Fig. 8), indicating that controlling factors of the carbonate system may not be exerted equally on both pH and pCO_2.

The extent of biological control on the system can also be investigated based on correlations between carbonate system parameters and dissolved oxygen (DO). Respiration-driven acidification is one of the most important local to regional contributors to acidification in coastal waters, with acidification closely linked to the widespread issue of deoxygenation (Rabalais et al., 2014; Strong et al., 2014). There were no observations of hypoxia at our study site during our monitoring, with minimum DO levels of 3.9 mg L^{-1} and 4.0 mg L^{-1} for our continuous monitoring period and our discrete sampling period, respectively. Despite the lack of hypoxia, there was a strong relationship between the carbonate system parameters and DO (Table 6), suggesting that

https://doi.org/10.5194/bg-2021-19
Preprint. Discussion started: 1 February 2021
© Author(s) 2021. CC BY 4.0 License.


net ecosystem metabolism may exert an important control on the carbonate system on certain time scales.

There was no significant difference in daytime and nighttime DO during any season (paired t-tests, winter p = 0.1573, spring p = 0.4877, summer p = 0.794) despite the significant differences in pH and pCO_2 between daytime and nighttime (Table 2). This suggests that net community metabolism is likely not a strong controlling factor of carbonate system parameters at this site on a diel time scale. The control exerted on the carbonate system by biological processes is likely much greater on the seasonal scale than the diel scale. The correlation between continuous pCO_2 and DO is stronger than pCO_2 and temperature, which suggests strong biological control and supports the indication by T/B values that non-thermal processes exert more control on pCO_2 than temperature. Both types of sampling (i.e., continuous and discrete) demonstrate that pH is generally highest in the winter and lowest in the summer and pCO_2 is highest in the summer and lowest in the winter (Figs. 2, and 3, Table 1). Though this seasonal pattern corresponds with the directional response from temperature fluctuations, it can also be explained by biological activity.

Given that this sampling location is in a ship channel where boat traffic (including large oil tankers) is relatively heavy, there is potential for atmospheric deposition of acids (SOx and NOx) to play a role in the carbonate system variability (Doney et al. 2007, Hunter et al. 2011). To try to understand this control, we deployed air samplers at our study site for eight 2-week periods. The levels of atmospheric NO_2 and SO_2 did not vary widely over the time period. NO_2 was ranged 5.45 to 6.99 ppb (6.13 ± 0.63 ppb), and SO_2 ranged 1.15 to 1.18 ppb (1.43 ± 0.35 ppb) over the sampling dates (J. D. Felix, personal

https://doi.org/10.5194/bg-2021-19
Preprint. Discussion started: 1 February 2021
© Author(s) 2021. CC BY 4.0 License.


communications). There was no apparent correlation between these values and the pH or pCO_2 levels over the 2-week sampling periods.

Co-locating our pH and pCO_2 sensors with other coastal environmental monitoring sensors allowed insight into correlated environmental parameters and potential driving forces of carbonate chemistry on diel and seasonal time scales. The results of this study provide strong support for the continued implementation of carbonate chemistry monitoring in conjunction with preexisting coastal environmental monitoring infrastructure. Our understanding of any estuarine system could benefit from long-term effective deployments of these monitoring tools. Strategically locating carbonate chemistry sensors at estuarine sites that are subject to local OA drivers or support large biodiversity or commercially important species may be the most crucial in guiding future mitigation and adaptation strategies for natural systems and aquaculture facilities (Chan et al., 2013; Strong et al., 2014).

4.2 Carbonate chemistry as a component of overall estuarine system variability

Estuaries and coastal areas are dynamic systems with human influence, riverine influence, and influence from an array of biogeochemical processes, resulting in highly variable chemical and environmental conditions. To better understand overall system variability over different time scales, we used a linear discriminant (LD) analysis, a multivariate statistic that allows dimensional reduction, to determine the linear combination of environmental parameters (individual parameters reduced into linear discriminants, LDs) that allow the best differentiation between day and night as well as between seasons. This used the same suite of environmental data and data sources as Sect. 4.1.2.

https://doi.org/10.5194/bg-2021-19
Preprint. Discussion started: 1 February 2021
© Author(s) 2021. CC BY 4.0 License.


All variables were centered and scaled to allow direct comparison of their contribution to the system variability. The magnitude (absolute value) of coefficients of the LDs (Table 7) represents the relative importance of each individual environmental parameter in the best discrimination between day and night and between seasons, i.e., the greater the absolute value of the coefficient, the more information the associated parameter can provide about whether the sample came from day or night (or winter, spring, or summer). Only one LD could be created for the diel variability (since there are only two classes to discriminate between – day and night). Two LDs could be created for the seasonal variability (since there were three classes to discriminate between – fall was omitted because of the lack of tidal data), but only the coefficients for LD1 are reported (Table 7) given that LD1 captured 95.64% of the seasonal variability.

Table 7. Coefficients of linear discriminants (LD) from discriminant function analysis (DFA) using continuous sensor data and other environmental parameters. Results for discriminants for both diel and seasonal variability shown. All variables were centered and scaled. For the seasonal analysis, only LD1 is given since it was captured 95.64% of the variability (for the diel analysis, there is only one . Given that many of the water quality parameters were measured in bottom waters and our sensors were measuring surface waters, only those observations without significant stratification in the water column (a salinity difference of less than 3 between surface and bottom) were included in these analyses.

	Diel	**Seasonal**
	LD1	**LD1**
Temperature (°C)	0.5406	-3.5279
Salinity	0.1473	0.0432
pCO_2 (µatm)	-0.1612	-0.2928
pH	0.0593	0.0991
Tide Level (m)	0.0968	-0.2389
Wind speed (ms^{-1})	-0.0009	0.0504
Total PAR	-2.2878	-0.0676
DO ($mg\ L^{-1}$)	-0.0839	0.0859
Turbidity	-0.0561	0.1455
Fluor. Chlorophyll	0.1397	-0.4040

As would be expected, we found that PAR provided the most differentiation between daytime and nighttime conditions (based on the largest coefficient associated

https://doi.org/10.5194/bg-2021-19
Preprint. Discussion started: 1 February 2021
© Author(s) 2021. CC BY 4.0 License.


772 with Diel LD1, Table 7). Temperature was the second most important factor in
773 differentiating between day and night; this corresponds to the diel variability that we
774 detected where both summer and fall had clear separation of mean temperature between
775 day and night, with nighttime temperatures being 0.3 and 1.0 higher, respectively (Table
776 3). The next most important parameter in differentiating between day and night in this
777 system was pCO_2, providing more evidence for differentiation between day and night
778 than other parameters that would be expected to vary on a diel timescale (e.g. chlorophyll
779 and DO). As for system variability that allowed differentiation between the four seasons,
780 the most important parameter in system variability was temperature (Table 7, Seasonal
781 LD1), as would be expected with the clear seasonal temperature fluctuations (Fig. 2E).
782 The second most important parameter in contributing to seasonal variability was
783 chlorophyll, likely indicating clear seasonal blooms. The third most important parameter
784 for seasonal differentiation was pCO_2; therefore pCO_2 variability seems to be more
785 closely tied to seasons than variability in tide level, DO, or the array of other parameters
786 (Table 7).

787 The contribution of pH to discriminating along diel or seasonal scales was less
788 than pCO_2 despite the same seasonal differences that were identified by ANOVA (Table
789 3) and more seasons with significant diel differences (Table 2). However, pH still seemed
790 to be relatively important on seasonal scales, having clearer contribution to seasonal
791 system variability than several other parameters including DO and salinity.

792 We can conclude that carbonate chemistry parameters are among the most
793 important of variants on both daily and seasonal time scales in this coastal setting.
794 Compared to six other estuaries around the United States with similar sensor deployments

https://doi.org/10.5194/bg-2021-19
Preprint. Discussion started: 1 February 2021
© Author(s) 2021. CC BY 4.0 License.


795 for carbonate chemistry characterization, our study site has a relatively small range of pH
796 and pCO_2 on both diel and seasonal scales (N. Rosenau, personal communication). While
797 we do not have the same suite of environmental data for these other systems, this
798 suggests that the relative amount of system variability contributed by carbonate chemistry
799 may be even greater in other estuarine systems. The relatively small fluctuations in pH
800 and pCO_2 that are seen on a daily scale at the Aransas Ship Channel is likely due to the
801 subtropical setting with little ocean upwelling influence and the lower estuary position of
802 our monitoring (further removed from the already small freshwater influence), but it may
803 also be tied to the system's relatively high buffer capacity. Just as the extent of hypoxia-
804 induced acidification was relatively low in Corpus Christi Bay compared to other systems
805 because of the bay's high buffer capacity (McCutcheon et al., 2019), the extent of pH
806 fluctuation on a daily scale from biological activity would also be modulated by the
807 intrinsic buffer capacity, which is likely also high in this system due to high alkalinity in
808 the freshwater endmembers (Yao et al., 2020).

809 *4.3 Comparing continuous monitoring and discrete sampling*

810 *4.3.1 Representative sampling in a temporally variable environment*

811 Discrete water sample collection and analysis is the most common method that
812 has been employed to attempt to understand the carbonate system of estuaries. However,
813 it is difficult to know if these samples are representative of the spatial and temporal
814 variability in carbonate system parameters. While this time-series study cannot conclude
815 whether our broader sampling efforts in the MAE are representative of the spatial
816 variability in the estuary, it can investigate how representative our bimonthly to monthly

https://doi.org/10.5194/bg-2021-19
Preprint. Discussion started: 1 February 2021
© Author(s) 2021. CC BY 4.0 License.


817 sampling is of the more high-frequency temporal variability that the Aransas Ship
818 Channel experiences.

819 One-way ANOVAs were conducted to compare between monitoring methods
820 (separate one-way ANOVAs within each season because of the significant interaction
821 between these factors in an initial two-way ANOVA). There were three levels of
822 monitoring method included in the comparison of means: continuous monitoring, discrete
823 monitoring during only the continuous monitoring period, and discrete monitoring over
824 the entire period (C, D_C, and D, respectively, in Table 3). To interpret the results, a
825 difference in means between the continuous monitoring and discrete monitoring datasets
826 would only indicate that the 10-month period of continuous monitoring was not
827 representative of the 5+ year period that discrete samples have been collected, but a
828 difference in means between the continuous data and discrete sample data collected
829 during the continuous monitoring period represents discrepancies between types of
830 monitoring.

831 There were several instances where seasonal parameter means significantly
832 differed between the 10-month continuous monitoring period and the 5+ year discrete
833 sampling period (Table 3, $C \neq D$ or $D_c \neq D$) including temperature in the summer and fall,
834 salinity in the spring, pH in the summer and fall, and pCO_2 in winter, spring, and summer.
835 While clear seasonal variability was demonstrated for most parameters (using both
836 continuous and discrete data for the entire period), these differences between the 10-
837 month continuous monitoring period and our 5+ year monitoring period illustrate that
838 there is also interannual variability in the system. Therefore, short periods of monitoring
839 are unable to fully capture current baseline conditions.

https://doi.org/10.5194/bg-2021-19
Preprint. Discussion started: 1 February 2021
© Author(s) 2021. CC BY 4.0 License.


840 During the continuous monitoring period (2016-2017), we found no significant
841 difference between sampling methods in the seasonal mean temperature, salinity, or
842 pCO_2. The two sampling methods also resulted in the same mean pH for all seasons
843 except for summer, when the sensor data recorded a higher mean pH than discrete
844 samples (Tables 1 and 3). During this case, we can conclude that discrete monitoring did
845 not accurately represent the system variability that was able to be captured by the sensor
846 monitoring. However, given that most seasons did not show differences in pH or pCO_2
847 between sampling methods, the descriptive statistics associated with the discrete
848 monitoring did a fair job of representing system means. This is evidence that long-term
849 discrete monitoring efforts, which are much more widespread in estuarine systems than
850 sensor deployments, can be generally representative of the system despite known
851 temporal variability on shorter time scales.
852 Understanding the relationships of pH and pCO_2 with temperature and salinity is
853 important in a system. Both the continuous and discrete sampling types indicate that pH
854 has a significant negative relationship with both temperature and salinity and pCO_2 has a
855 s significant positive relationship with both temperature and salinity (Fig. 7). Based on
856 the results of an Analysis of Covariance (ANCOVA), the relationship (slope) of pH with
857 both temperature and salinity and of pCO_2 with salinity were not significantly different
858 between types of monitoring (considering the sensor deployment period only), supporting
859 the effectiveness of long-term discrete monitoring programs when sensors are unable to
860 be deployed. However, ANCOVA did reveal the relationship of pCO_2 with temperature is
861 significantly different (method:temp p=0.0062) between monitoring methods.

https://doi.org/10.5194/bg-2021-19
Preprint. Discussion started: 1 February 2021
© Author(s) 2021. CC BY 4.0 License.


While *in situ* monitoring is usually lacking good spatial coverage, it is effective in capturing temporal resolution and presumably providing better estimates of average CO_2 flux at a given location versus periodic sampling. Previous studies have pointed out that discrete sampling methods, which generally involve only daytime sampling, do not adequately capture the diel variability in the carbonate system and may therefore lead to underestimation of CO_2 fluxes. However, we found no significant difference (within any season) between CO_2 flux values calculated with sensor data versus discrete samples (Table 3). Calculated CO_2 fluxes also did not significantly differ between day and night during any season, despite some differences in pCO_2 (Table 2), likely due to the large error associated with the calculation of CO_2 flux (Table 1, Fig. 5) which will be further discussed below. Therefore, the expected underestimation of CO_2 flux based on diel variability of pCO_2 was not encountered at our study site, validating the use of discrete samples for quantification of CO_2 fluxes (until methods with less associated error are available). Even given less error in calculated flux, estimated fluxes would likely not differ between methods on an annual scale (as pCO_2 did not), but CO_2 fluxes may differ on a seasonal scale since the differences between daytime and nighttime pCO_2 were not consistent across seasons (Table 2).

There are many factors contributing to error associated with CO_2 flux. There is still large error associated with estimates of estuarine CO_2 flux because turbulent mixing is difficult to model and turbulence is the main control on CO_2 gas transfer velocity, k, in shallow water environments. Thus, our wind speed parameterization of k is imperfect and likely the greatest source of error. Other notable sources of error include the data treatment. For example, we chose to seasonally weight the individual calculated flux

https://doi.org/10.5194/bg-2021-19
Preprint. Discussion started: 1 February 2021
© Author(s) 2021. CC BY 4.0 License.


values in the calculation of annual flux to account for differences in sampling frequency between seasons. From continuous data, the weighted average flux was 0.2 mmol m^{-2} d^{-1}, although choosing not to seasonally weight and simply look at the arithmetic mean of fluxes calculated directly from sampling dates would have resulted in an annual CO_2 flux of -0.7 mmol m^{-2} d^{-1} for the same period. Similarly, the weighted average flux from all 5+ years of discrete data was -0.9 mmol m^{-2} d^{-1}, but the arithmetic mean of fluxes would have resulted in an annual CO_2 flux of 0.2 mmol m^{-2} d^{-1} for the same period. Another source of error that could be associated with the calculation of flux from the discrete data is the way in which wind speed data are aggregated to be used in the windspeed parameterization. We decided to use daily averages of the windspeed for calculations. Using the windspeed measured for the closest time to our sampling time or the monthly averaged wind speed may have resulted in very different flux values.

4.3.2 Direct agreement of measurement methods and quantified uncertainties associated with parameters

Direct comparisons were made between measurements from sensors and laboratory-analyzed bottle samples—including both quality control (QC) samples taken from the cooler that housed the sensors at the time when these sensors took recorded readings and long-term monitoring samples taken from the ship channel near the sensors (within 100 m) that occurred at various times and were compared to sensor measurements of the closest full hour (Table 8). The mean difference between the SeaFET pH measurements and the QC samples (continuous – discrete) prior to sensor data correction was 0.05 ± 0.08 (Table 8, which would reduce to 0.00 ± 0.08 following the correction). The mean difference between the SAMICO2 pCO_2 measurements and the QC samples

https://doi.org/10.5194/bg-2021-19
Preprint. Discussion started: 1 February 2021
© Author(s) 2021. CC BY 4.0 License.

908 (continuous – discrete) was -18 ± 44 (Table 8) when discrete sample pCO_2 was calculated
909 using Millero (2010) constants. We used several different constants to calculate pCO_2 to
910 check this offset; all were similar in mean and standard deviation, but the offset could be
911 slightly reduced using Millero (2002) constants.

912 Table 8. Comparison of discrete and continuous monitoring. The difference between
913 sampling methods is reported in two different ways: the difference between sensor
914 measurements and laboratory measurement of quality control (QC) bottle samples taken
915 directly from the cooler (here the pH difference is prior to the sensor pH correction of
916 +0.05), and the difference between sensor measurements and laboratory measurement of
917 bottle samples taken from a nearby station for our 5+ year monitoring (here the pH
918 difference if after the sensor pH correction of +0.05, see methods for details). For all
919 calculated parameters, dissociation constants from Millero 2010 were used. Error—
920 analytical error for directly measured parameters and propagated error for calculated
921 parameters (mean ± standard deviation, calculated in the seacarb package in R—
922 associated with carbonate system variables is also reported.

	Difference between sampling methods (mean difference ± standard deviation of the difference)		Error (Analytical or Propagated)	
	Sensor – QC cooler samples (prior to sensor pH correction, n=12)	Sensor – discrete samples (after pH sensor correction, n=13)	**Discrete Sampling (n = 104)**	**Continuous Monitoring (n = 6088)**
Temperature (°C)			0.1	0.1
Salinity	-0.16 ± 1.44	0.50 ± 1.69	0.01	0.1
pH	-0.05 ± 0.08	0.01 ± 0.12	0.0004	0.05
pCO_2 (µatm)	-18 ± 44	25 ± 63	7 ± 2	1.0
DIC (µmol kg^{-1})			±2.5	327.4 ± 63.2
TA (µmol kg^{-1})			7.4 ± 0.9	400.7 ± 81.0
Ω_{Ar}			0.19 ± 0.03	1.08 ± 0.31

923

924 Given that the analytical accuracy of the SeaFET instrument is 0.05 pH units, the
925 average offset between sensor and laboratory values of quality control samples
926 demonstrates fair agreement (Table 8). Given that calculated uncertainty associated with
927 calculated discrete pCO_2 was 7 ± 2, we did not see great agreement between SAMICO2
928 pCO_2 and laboratory-calculated pCO_2 for quality control samples (mean difference of -18
929 ± 44, Table 8). Mean offsets and their associated standard deviations were larger when

https://doi.org/10.5194/bg-2021-19
Preprint. Discussion started: 1 February 2021
© Author(s) 2021. CC BY 4.0 License.


930 comparing sensor data to samples taken during our long-term discrete monitoring effort.
931 This is not surprising given that the discrete sample collection did not occur at the exact
932 time of the sensor measurement or the exact location of the cooler pump inlet. Greater
933 sensor-laboratory agreement has been achieved for open ocean settings, but this larger
934 standard deviation is likely a result of the temporal variability in the more complex
935 estuarine environment where these instruments have been much less widely deployed to
936 date.

937 Propagation of error associated with computed carbonate system parameters was
938 done using the *seacarb* package in R (Gattuso et al., 2018); the error propagation includes
939 error associated with the measurements of the input pair (1 µatm for pCO_2 from
940 SAMICO2 and 0.05 for pH from SeaFET; 0.0004 for laboratory spectrophotometric pH
941 and 2.5 µmol kg^{-1} for laboratory DIC), error associated with *in-situ* temperature (0.1 °C)
942 and salinity (0.1 for sensor-measured and 0.01 for laboratory-measured), and error
943 associated with total boron the key dissociation constants (standard recommended error
944 used) (Table 8). While the error associated with calculated parameters from discrete
945 bottle samples was relatively small and likely a result of uncertainties in constants (Orr et
946 al., 2018), we note that the error associated with calculated dissolved inorganic carbon
947 (DIC), total alkalinity (TA), and saturation state of aragonite (Ω_{Ar}), which are other
948 frequently addressed carbonate system parameters, was large when calculated with sensor
949 data. This large error is likely a result of both the relatively low analytical precision
950 associated with the pH sensor and the poor mathematical combination of variables for
951 speciation calculations. Hence, we limited the discussion to pH (which was directly
952 measured for both continuous monitoring and laboratory analysis of discrete samples)

https://doi.org/10.5194/bg-2021-19
Preprint. Discussion started: 1 February 2021
© Author(s) 2021. CC BY 4.0 License.


and pCO_2 (which was directly measured for continuous monitoring and had relatively low error when calculated with discrete sample DIC and pH, Table 8) and omitted any discussion of the parameters with high propagation error. The high error suggests that it may be important to develop and broadly use autonomous sensors that can measure carbonate system parameters that allow for lower propagated error to have a full picture of estuarine carbonate chemistry on high-frequency time scales.

5. Conclusions

We monitored carbonate chemistry parameters (pH and pCO_2) using both sensor deployments (10 months) and discrete sample collection (5+ years) at the Aransas Ship Channel, TX, to characterize temporal variability and investigate controlling factors. Both sampling methods demonstrated significant seasonal variability at the location, with highest pH (lowest pCO_2) in the winter and lowest pH (highest pCO_2) in the summer. Significant diel variability was also evident from sensor data, though diel fluctuations were smaller than many other areas previously studied. Carbonate chemistry parameters were among the most important environmental parameters to distinguish between both diel and seasonal environmental conditions.

The difference between daytime and nighttime values of carbonate system parameters varied between seasons, occasionally reversing the expected diel variability due to biological processes. It was evident that biological activity is not the strongest controlling factor of diel variability at this location, likely surpassed by tidal control despite the small tidal range in the northwestern GOM. Controls on the system also differed over different time scales, with temperature becoming a less important control over shorter time scales.

https://doi.org/10.5194/bg-2021-19
Preprint. Discussion started: 1 February 2021
© Author(s) 2021. CC BY 4.0 License.


976 Tides exerted significant control on the carbonate system, and low tide allowed
977 more biological control of the system. Higher mean pCO_2 was reported for low tide
978 versus high tide across all seasons. pH was higher at high tide during winter and summer
979 but deviated from the expected pattern during spring with lower pH during high tide. The
980 results suggest that the controlling factors of the carbonate system may not be exerted
981 equally on both pH and pCO_2 on diel timescales, causing separation of their diel or tidal
982 relationships during certain seasons. The detailed investigation of controlling factors
983 provides strong support for the implementation of carbonate chemistry monitoring in
984 conjunction with preexisting coastal environmental monitoring infrastructure, which has
985 had little application in estuarine environments thus far.
986 Despite known temporal variability on shorter timescales, discrete sampling was
987 generally representative of the average carbonate system on a seasonal and annual basis
988 based on comparison with our sensor data. Additionally, there was no difference in CO_2
989 flux between sampling types supporting the validity of discrete sample collection for
990 carbonate system characterization.

991 **Data availability**

992 Continuous sensor data are archived with the National Oceanic and Atmospheric
993 Administration's (NOAA's) National Centers for Environmental Information (NCEI)
994 (https://doi.org/10.25921/dkg3-1989). Discrete sample data are available in two separate
995 datasets archived with National Science Foundation's Biological & Chemical
996 Oceanography Data Management Office (BCO-DMO) (doi:10.1575/1912/bco-
997 dmo.784673.1 and doi: 10.26008/1912/bco-dmo.835227.1).

https://doi.org/10.5194/bg-2021-19
Preprint. Discussion started: 1 February 2021
© Author(s) 2021. CC BY 4.0 License.


998 **Author Contribution**

999 MM and XH defined the scope of this work. XH received funding for all components of
1000 the work. MM, HY, and CJS performed field sampling and laboratory analysis of
1001 samples. MM prepared the initial manuscript and all co-authors contributed to revisions.

1002 **Competing interests**

1003 The authors declare that they have no conflict of interest.

1004

1005 **Acknowledgements**

1006 Funding for autonomous sensors and sensor deployment was provided by the
1007 United States Environmental Protection Agency's National Estuary Program via the
1008 Coastal Bend Bays and Estuaries Program Contract No. 1605 Thanks to Rae Mooney
1009 from Coastal Bend Bays and Estuaries Program for assistance in the initial sensor setup.
1010 Funding for discrete sampling as well MM's dissertation research has been supported by
1011 both NOAA National Center for Coastal Ocean Science (Contract No.
1012 NA15NOS4780185) and NSF Chemical Oceanography Program (OCE-1654232). We
1013 also appreciate the support from the Mission-Aransas National Estuarine Research
1014 Reserve in allowing us the boat-of-opportunity for our ongoing discrete sample
1015 collections and the University of Texas Marine Science Institute for allowing us access to
1016 their research pier for the sensor deployment. A special thanks to Hongjie Wang, Lisette
1017 Alcocer, Allen Dees, and Karen Alvarado for assistance with field work.

1018 **References**

1019 Barton, A., Waldbusser, G.G., Feely, R.A., Weisberg, S.B., Newton, J.A., Hales, B.,
1020 Cudd, S., Eudeline, B., Langdon, C.J., Jefferds, I., King, T., Suhrbier, A.,

https://doi.org/10.5194/bg-2021-19
Preprint. Discussion started: 1 February 2021
© Author(s) 2021. CC BY 4.0 License.


1021 Mclaughlin, K., 2015. Impacts of Coastal Acidification on the Pacific Northwest
1022 Shellfish Industry and Adaptation Strategies Implemented in Response.
1023 Oceanography 28, 146–159.
1024 Bednaršek, N., Tarling, G.A., Bakker, D.C.E., Fielding, S., Jones, E.M., Venables, H.J.,
1025 Ward, P., Kuzirian, A., Lézé, B., Feely, R.A., Murphy, E.J., 2012. Extensive
1026 dissolution of live pteropods in the Southern Ocean. Nat. Geosci. 5, 881–885.
1027 https://doi.org/10.1038/ngeo1635
1028 Borges, A. V., 2005. Do We Have Enough Pieces of the Jigsaw to Integrate CO2 Fluxes
1029 in the Coastal Ocean ? Estuaries 28, 3–27.
1030 Bruesewitz, D. a., Gardner, W.., Mooney, R.F., Pollard, L., Buskey, E.J., 2013. Estuarine
1031 ecosystem function response to flood and drought in a shallow, semiarid estuary:
1032 Nitrogen cycling and ecosystem metabolism. Limnol. Oceanogr. 58, 2293–2309.
1033 https://doi.org/10.4319/10.2013.58.6.2293
1034 Caffrey, J.M., 2004. Factors controlling net ecosystem metabolism in U.S. estuaries.
1035 Estuaries 27, 90–101. https://doi.org/10.1007/BF02803563
1036 Cai, W.-J., 2011. Estuarine and Coastal Ocean Carbon Paradox: CO_2 Sinks or Sites of
1037 Terrestrial Carbon Incineration? Ann. Rev. Mar. Sci. 3, 123–145.
1038 https://doi.org/10.1146/annurev-marine-120709-142723
1039 Cai, W.-J., Hu, X., Huang, W.-J., Murrell, M.C., Lehrter, J.C., Lohrenz, S.E., Chou, W.-
1040 C., Zhai, W., Hollibaugh, J.T., Wang, Y., Zhao, P., Guo, X., Gundersen, K., Dai, M.,
1041 Gong, G.-C., 2011. Acidification of subsurface coastal waters enhanced by
1042 eutrophication. Nat. Geosci. 4, 766–770. https://doi.org/10.1038/ngeo1297
1043 Carstensen, J., Chierici, M., Gustafsson, B.G., Gustafsson, E., 2018. Long-Term and

© Author(s) 2021. CC BY 4.0 License.


1044 Seasonal Trends in Estuarine and Coastal Carbonate Systems. Global Biogeochem.
1045 Cycles 1271–1288. https://doi.org/10.1002/2017GB005699
1046 Challener, R.C., Robbins, L.L., McClintock, J.B., 2015. Variability of the carbonate
1047 chemistry in a shallow , seagrass-dominated ecosystem : implications for ocean
1048 acidification experiments. Mar. Freshw. Res.
1049 Chan, F., A.B., B., Barth, J.A., Chornesky, E.A., Dickson, A.G., Feely, R.A., Hales, B.,
1050 Hill, T.M., Hofmann, G., Ianson, D., Klinger, T., Largier, J., Newton, J., Pedersedn,
1051 T.F., Somero, G.N., Sutula, M., Wakefield, W.W., Walkdbusser, G.G., Weisberg,
1052 S.B., Whiteman, E.., 2013. The West Coast Ocean Acidification and Hypoxia
1053 Science Panel: Major Findings, Recommendations, and Actions, California Ocean
1054 Science Trust.
1055 Crosswell, J.R., Anderson, I.C., Stanhope, J.W., Van Dam, B., Brush, M.J., Ensign, S.,
1056 Piehler, M.F., McKee, B., Bost, M., Paerl, H.W., 2017. Carbon budget of a shallow,
1057 lagoonal estuary: Transformations and source-sink dynamics along the river-estuary-
1058 ocean continuum. Limnol. Oceanogr. 62, S29–S45.
1059 https://doi.org/10.1002/lno.10631
1060 Cyronak, T., Andersson, A.J., D'Angelo, S., Bresnahan, P., Davidson, C., Griffin, A.,
1061 Kindeberg, T., Pennise, J., Takeshita, Y., White, M., 2018. Short-Term Spatial and
1062 Temporal Carbonate Chemistry Variability in Two Contrasting Seagrass Meadows:
1063 Implications for pH Buffering Capacities. Estuaries and Coasts 41, 1282–1296.
1064 https://doi.org/10.1007/s12237-017-0356-5
1065 Dickson, A.G., 1990. Standard potential of the reaction: AgCl(s) + 1 2H2(g) = Ag(s) +
1066 HCl(aq), and and the standard acidity constant of the ion HSO4- in synthetic sea

https://doi.org/10.5194/bg-2021-19
Preprint. Discussion started: 1 February 2021
© Author(s) 2021. CC BY 4.0 License.


1067 water from 273.15 to 318.15 K. J. Chem. Thermodyn. 22, 113–127.
1068 https://doi.org/10.1016/0021-9614(90)90074-Z
1069 Ekstrom, J. a., Suatoni, L., Cooley, S.R., Pendleton, L.H., Waldbusser, G.G., Cinner, J.E.,
1070 Ritter, J., Langdon, C., van Hooidonk, R., Gledhill, D., Wellman, K., Beck, M.W.,
1071 Brander, L.M., Rittschof, D., Doherty, C., Edwards, P.E.T., Portela, R., 2015.
1072 Vulnerability and adaptation of US shellfisheries to ocean acidification. Nat. Clim.
1073 Chang. 5, 207–214. https://doi.org/10.1038/nclimate2508
1074 Gattuso, J.-P., Frankignoulle, M., Wollast, R., 1998. Carbon and Carbonate Metabolism
1075 in Coastal Aquatic Ecosystems. Annu. Rev. Ecol. Syst. 29, 405–434.
1076 https://doi.org/10.1146/annurev.ecolsys.29.1.405
1077 Gattuso, J.P., Epitalon, J.M., Lavigne, H., Orr, J.C., 2018. seacarb seawater carbonate
1078 chemistry with R, R package version 3.2.8.
1079 Gazeau, F., Quiblier, C., Jansen, J.M., Gattuso, J.-P., Middelburg, J.J., Heip, C.H.R.,
1080 2007. Impact of elevated CO 2 on shellfish calcification. Geophys. Res. Lett. 34,
1081 L07603. https://doi.org/10.1029/2006GL028554
1082 Gobler, C.J., Talmage, S.C., 2014. Physiological response and resilience of early life-
1083 stage Eastern oysters (Crassostrea virginica) to past , present and future ocean
1084 acidification 2, 1–15. https://doi.org/10.1093/conphys/cou004.Introduction
1085 Ho, D.T., Law, C.S., Smith, M.J., Schlosser, P., Harvey, M., Hill, P., 2006.
1086 Measurements of air-sea gas exchange at high wind speeds in the Southern Ocean :
1087 Implications for global parameterizations 33, 1–6.
1088 https://doi.org/10.1029/2006GL026817
1089 Hofmann, G.E., Smith, J.E., Johnson, K.S., Send, U., Levin, L. a, Micheli, F., Paytan, A.,

© Author(s) 2021. CC BY 4.0 License.


1090 Price, N.N., Peterson, B., Takeshita, Y., Matson, P.G., Crook, E.D., Kroeker, K.J.,
1091 Gambi, M.C., Rivest, E.B., Frieder, C. a, Yu, P.C., Martz, T.R., 2011. High-
1092 frequency dynamics of ocean pH: a multi-ecosystem comparison. PLoS One 6,
1093 e28983. https://doi.org/10.1371/journal.pone.0028983
1094 Hsu S. A., 1994. Determining the Power-Law Wind-Profile Exponent under Near-Neatral
1095 Stability Condidtions at Sea. J. Appl. Meteorol. 33, 757–765.
1096 Hu, X. (2019) Carbonate chemistry effects from Hurricane Harvey in San Antonio Bay
1097 and Mission Aransas Estuary from 2017-02-22 to 2018-11-15. Biological and
1098 Chemical Oceanography Data Management Office (BCO-DMO). (Version 1)
1099 Version Date 2019-12-19. doi:10.1575/1912/bco-dmo.784673.1. Accessed [2021-
1100 01-28]
1101 Hu, X., Beseres Pollack, J., McCutcheon, M.R., Montagna, P. a., Ouyang, Z., 2015.
1102 Long-term alkalinity decrease and acidification of estuaries in Northwestern Gulf of
1103 Mexico. Environ. Sci. Technol. 49, 3401–3409. https://doi.org/10.1021/es505945p
1104 Hu, Xinping; McCutcheon, Melissa R. (2020). Sensor continuous measurements of pH,
1105 partial pressure of carbon dioxide (pCO2), salinity and temperature at the University
1106 of Texas Marine Science Institute Research Pier, Aransas Ship Channel, TX, Gulf of
1107 Mexico from 2016-11-08 to 2017-08-23 (NCEI Accession 0222572). NOAA
1108 National Centers for Environmental Information. Dataset.
1109 https://doi.org/10.25921/dkg3-1989. Accessed [2021-01-28]
1110 Hu, X., Nuttall, M.F., Wang, H., Yao, H., Staryk, C.J., McCutcheon, M.R., Eckert, R.J.,
1111 Embesi, J.A., Johnston, M.A., Hickerson, E.L., Schmahl, G.P., Manzello, D.,
1112 Enochs, I.C., DiMarco, S., Barbero, L., 2018. Seasonal variability of carbonate

© Author(s) 2021. CC BY 4.0 License.


chemistry and decadal changes in waters of a marine sanctuary in the Northwestern Gulf of Mexico. Mar. Chem. 205, 16–28. https://doi.org/10.1016/j.marchem.2018.07.006

Jiang, L.-Q., Cai, W.-J., Wang, Y., 2008. A comparative study of carbon dioxide degassing in river- and marine-dominated estuaries. Limnol. Oceanogr. 53, 2603–2615. https://doi.org/10.4319/lo.2008.53.6.2603

Jiang, L.Q., Cai, W.J., Wang, Y., Bauer, J.E., 2013. Influence of terrestrial inputs on continental shelf carbon dioxide. Biogeosciences 10, 839–849. https://doi.org/10.5194/bg-10-839-2013

Kealoha, A.K., Shamberger, K.E.F., DiMarco, S.F., Thyng, K.M., Hetland, R.D., Manzello, D.P., Slowey, N.C., Enochs, I.C., 2020. Surface Water CO2 variability in the Gulf of Mexico (1996–2017). Sci. Rep. 10, 1–13. https://doi.org/10.1038/s41598-020-68924-0

Laruelle, G.G., Cai, W.-J., Hu, X., Gruber, N., Mackenzie, F.T., Regnier, P., 2018. Continental shelves as a variable but increasing global sink for atmospheric carbon dioxide. Nat. Commun. 9, 454. https://doi.org/10.1038/s41467-017-02738-z

Li, D., Chen, J., Ni, X., Wang, K., Zeng, D., Wang, B., Jin, H., Huang, D., Cai, W.-J., 2018. Effects of biological production and vertical mixing on sea surface p CO 2 variations in the Changjiang River plume during early autumn: A buoy-based time series study. J. Geophys. Res. Ocean. 123, 6156–6173. https://doi.org/10.1029/2017JC013740

Mathis, J.T., Pickart, R.S., Byrne, R.H., Mcneil, C.L., Moore, G.W.K., Juranek, L.W., Liu, X., Ma, J., Easley, R.A., Elliot, M.M., Cross, J.N., Reisdorph, S.C., Bahr, F.,

https://doi.org/10.5194/bg-2021-19
Preprint. Discussion started: 1 February 2021
© Author(s) 2021. CC BY 4.0 License.


1136 Morison, J., Lichendorf, T., Feely, R.A., 2012. Storm-induced upwelling of high p
1137 CO 2 waters onto the continental shelf of the western Arctic Ocean and implications
1138 for carbonate mineral saturation states 39, 4–9.
1139 https://doi.org/10.1029/2012GL051574
1140 McCutcheon, M. R., Hu, X. (2021) Carbonate chemistry in Mission Aransas Estuary
1141 from May 2014 to Feb 2017 and Dec 2018 to Feb 2020. Biological and Chemical
1142 Oceanography Data Management Office (BCO-DMO). (Version 1) Version Date
1143 2021-01-04. http://lod.bco-dmo.org/id/dataset/835227. Accessed [2021-01-28]
1144 McCutcheon, M.R., Staryk, C.J., Hu, X., 2019. Characteristics of the Carbonate System
1145 in a Semiarid Estuary that Experiences Summertime Hypoxia. Estuaries and Coasts.
1146 https://doi.org/10.1007/s12237-019-00588-0
1147 Millero, F.J., 2010. Carbonate constant for estuarine waters. Mar. Freshw. Res. 61, 139–
1148 142.
1149 Montagna, P. a, Brenner, J., Gibeaut, J., Morehead, S., 2011. Chapter 4: Coastal Impacts,
1150 in: Jurgen Schmandt, Gerald R. North, and J.C. (Ed.), The Impact of Global
1151 Warming on Texas. University of Texas Press, pp. 96–123.
1152 Orr, J.C., Epitalon, J.-M., Dickson, A.G., Gattuso, J.-P., 2018. Routine uncertainty
1153 propagation for the marine carbon dioxide system. Mar. Chem.
1154 https://doi.org/10.1016/j.marchem.2018.10.006
1155 Rabalais, N.N., Cai, W.-J., Carstensen, J., Conley, D.J., Fry, B., Hu, X., Quinones-
1156 Rivera, Z., Rosenberg, R., Slomp, C.P., Turner, R.E., Voss, M., Wissel, B., Zhang,
1157 J., 2014. Eutrophication-driven Deoxygenation in the Coastal Ocean. Oceanography
1158 27, 172–183.

https://doi.org/10.5194/bg-2021-19
Preprint. Discussion started: 1 February 2021
© Author(s) 2021. CC BY 4.0 License.


1159 Raymond, P. a., Cole, J.J., 2001. Gas Exchange in Rivers and Estuaries: Choosing a Gas
1160 Transfer Velocity. Estuaries 24, 312. https://doi.org/10.2307/1352954
1161 Robbins, L.L., Lisle, J.T., 2018. Regional Acidification Trends in Florida Shellfish
1162 Estuaries: a 20+ Year Look at pH, Oxygen, Temperature, and Salinity. Estuaries and
1163 Coasts 41, 1268–1281. https://doi.org/10.1007/s12237-017-0353-8
1164 Sastri, A.R., Christian, J.R., Achterberg, E.P., Atamanchuk, D., Buck, J.J.H., Bresnahan,
1165 P., Duke, P.J., Evans, W., Gonski, S.F., Johnson, B., Juniper, S.K., Mihaly, S.,
1166 Miller, L.A., Morley, M., Murphy, D., Nakaoka, S.I., Ono, T., Parker, G., Simpson,
1167 K., Tsunoda, T., 2019. Perspectives on in situ Sensors for Ocean Acidification
1168 Research. Front. Mar. Sci. 6, 1–6. https://doi.org/10.3389/fmars.2019.00653
1169 Schulz, K.G., Riebesell, U., 2013. Diurnal changes in seawater carbonate chemistry
1170 speciation at increasing atmospheric carbon dioxide. Mar. Biol. 160, 1889–1899.
1171 https://doi.org/10.1007/s00227-012-1965-y
1172 Seim, H.E., Kjerfve, B., Sneed, J.E., 1987. Tides of Mississippi Sound and the adjacent
1173 continental shelf. Estuar. Coast. Shelf Sci. 25, 143–156.
1174 https://doi.org/10.1016/0272-7714(87)90118-1
1175 Semesi, I.S., Beer, S., Björk, M., 2009. Seagrass photosynthesis controls rates of
1176 calcification and photosynthesis of calcareous macroalgae in a tropical seagrass
1177 meadow. Mar. Ecol. Prog. Ser. 382, 41–47. https://doi.org/10.3354/meps07973
1178 Solis, R.S., Powell, G.L., 1999. Hydrography, Mixing Characteristics, and Residence
1179 Time of Gulf of Mexico Estuaries.
1180 Strong, A.L., Kroeker, K.J., Teneva, L.T., Mease, L.A., Kelly, R.P., 2014. Ocean
1181 acidification 2.0: Managing our Changing Coastal Ocean Chemistry. Bioscience 64,

© Author(s) 2021. CC BY 4.0 License.


581–592. https://doi.org/10.1093/biosci/biu072

Thurman, H. V., 1994. Introductory Oceanography, seventh edition. pp. 252–276.

Uppström, L.R., 1974. The boron/chlorinity ratio of deep-sea water from the Pacific Ocean. Deep. Res. Oceanogr. Abstr. 21, 161–162. https://doi.org/10.1016/0011-7471(74)90074-6

USGS, 2001. Discharge Between San Antonio Bay and Aransas Bay, Southern Gulf Coast, Texas, May-September 1999.

Waldbusser, G.G., Salisbury, J.E., 2014. Ocean Acidification in the Coastal Zone from an Organism's Perspective: Multiple System Parameters, Frequency Domains, and Habitats. Ann. Rev. Mar. Sci. 6, 221–247. https://doi.org/10.1146/annurev-marine-121211-172238

Wanninkhof, R., 1992. Relationship Between Wind Speed and Gas Exchange. J. Geophys. Res. 97, 7373–7382. https://doi.org/10.1029/92JC00188

Wanninkhof, R., Asher, W.E., Ho, D.T., Sweeney, C., McGillis, W.R., 2009. Advances in quantifying air-sea gas exchange and environmental forcing. Ann. Rev. Mar. Sci. 1, 213–244. https://doi.org/10.1146/annurev.marine.010908.163742

Weiss, R.F., 1974. Carbon dioxide in water and seawater: the solubility of a non-ideal gas. Mar. Chem. 2, 203–215.

Westfall, P.H., 1997. Multiple Testing of General Contrasts Using Logical Constraints and Correlations. J. Am. Stat. Assoc. 92, 299–306. https://doi.org/10.1080/01621459.1997.10473627

Yao, H., Hu, X., 2017. Responses of carbonate system and CO2flux to extended drought and intense flooding in a semiarid subtropical estuary. Limnol. Oceanogr. 62, S112–

https://doi.org/10.5194/bg-2021-19
Preprint. Discussion started: 1 February 2021
© Author(s) 2021. CC BY 4.0 License.


S130. https://doi.org/10.1002/lno.10646

Yao, H., McCutcheon, M.R., Staryk, C.J., Hu, X., 2020. Hydrologic controls on CO2 chemistry and flux in subtropical lagoonal estuaries of the northwestern Gulf of Mexico. Limnol. Oceanogr. 1–19. https://doi.org/10.1002/lno.11394

Yates, K.K., Dufore, C., Smiley, N., Jackson, C., Halley, R.B., 2007. Diurnal variation of oxygen and carbonate system parameters in Tampa Bay and Florida Bay. Mar. Chem. 104, 110–124. https://doi.org/10.1016/j.marchem.2006.12.008